

**General Response: We thank the Referee#1 for your helpful comments. We have addressed all comments and provided point by point response below. The revised manuscript is presented in below Response**

- 1) This paper examines the composition of primary biological aerosol particles (PBAP) collected on various substrates for offline analysis, at a mountainous boreal forest site in China. Particles were classified optically based on morphology and composition was determined using a combination of TEM & EDS. The authors report that PBAP were found to contain key, unique compositional markers (e.g., elemental P), which is consistent with previous studies performing similar analysis. A key result of this study was demonstrating that 20% of bacterial particles were internally mixed with non-PBAP, which may have a significant impact on the long range transport of bacteria and aerosol budgets as well as mixed-phase aerosol-cloud interactions. The authors also examined PBAP hygroscopicity, demonstrating that the sampled PBAP display small growth factors and subsequently weak hygroscopicity. Overall the paper is reasonably well written and provides useful information to be absorbed into our general understanding of PBAP emissions and quantifying the fraction of PBAP which are internally mixed is a key result.

Response: We appreciated the referee's positive comments.

- 2) My only significant criticism is that the paper lacks detail on the sample/substrate handling procedure employed, what procedures were in place to minimise contamination and how any contamination was dealt with during analysis.

Response: We added some explanations about the sample/substrate here. In the section 2.1, we explained the sample storage that the Cu grids and silicon wafers placed in a dry, clean, and airtight container were stored in a desiccator at 25 °C and 20±3% RH to minimize exposure to ambient air and preserve them for analysis. Because the TEM can directly observe the dry samples, the procedures before the TEM analysis can guarantee no contamination. The method is widely used in many studies for individual particle analysis. We added one Figure S1 in the revised manuscript as below.

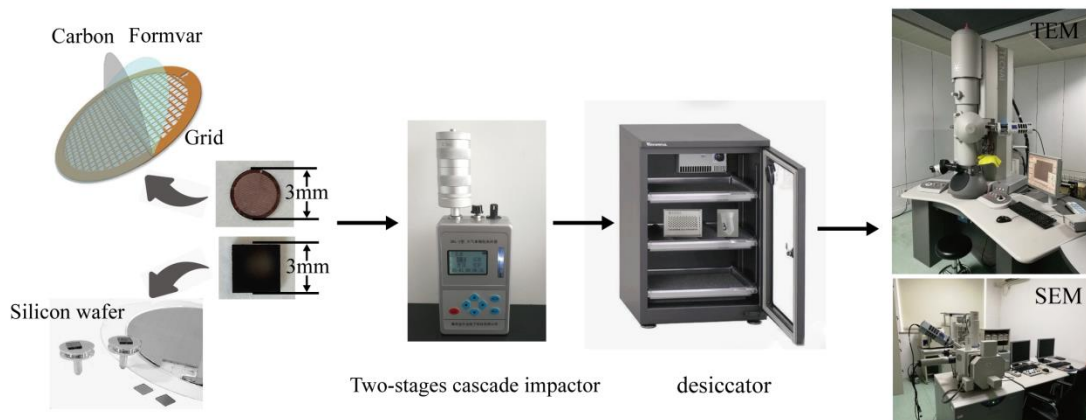


**Figure S1** The sampling procedures of substrate, sampler, storage, and analyzed technique.

To further confirm the procedure about the PBAPs, we obtained *Yeast* and *colibacillus* cultivated

in the laboratory (Figure 5 and S2). We found the TEM analysis were no problem to obtain morphology of bacteria and fungi.

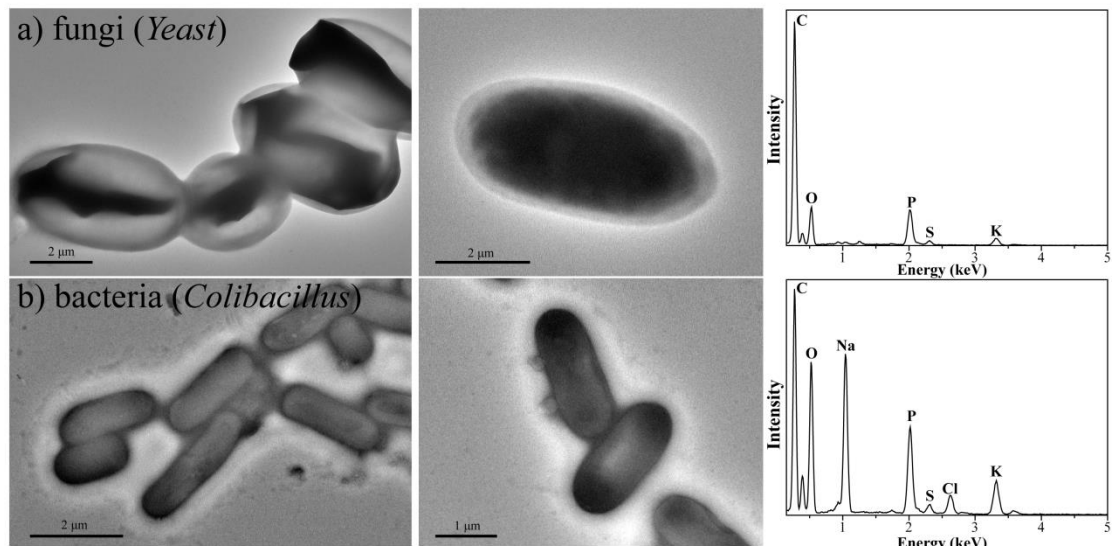


**Figure S2** The *Yeast* and the *colibacillus* particles cultivated in laboratory. TEM image showing morphology and EDS showing compositions.

As these two referee's requests, I added more explanations here to provide details about the sampling procedure and detailed analysis. We mainly revised the Method section, please read the RED words.

In context P154-163 "Individual particle samples were collected both on copper (Cu) TEM grids coated with carbon film (carbon type-B, 300-mesh copper; Tianld Co., China) and on silicon membranes (thickness:  $500\pm10\text{ }\mu\text{m}$ , size:  $3\times3\text{ mm}$ ; LIJINGKEJI, China) by a single-stage cascade impactor called the DKL-2 sampler (Genstar Electronic Technology, China). The collection efficiency of the impactor is 50% for particles with an aerodynamic diameter of  $0.1\text{ }\mu\text{m}$  when we assume an aerosol particle density of  $2\text{ g cm}^{-3}$ . We collected individual particles four times each day at 9:00, 15:00, 21:00, and 02:00 local time. At each sampling event, we first collected TEM grids and then changed to silicon wafers in the sampler. The sampling duration at each time varied from 10 min to 25 min depending on the particle distribution on the substrate. The substrates of the carbon film and silicon wafer both have smooth surfaces with no contamination before we use them to collect aerosol particles."

P144-149 "The distribution of aerosol particles on TEM grids was not uniform, with coarser particles occurring near the center and finer particles on the periphery. The quick check by the optical microscopy enabled us to tell whether individual particles were well distributed and whether there was any overlap on the substrate. Whenever the distribution was not even enough or when substantial overlap occurred, we had to discard it and re-collect individual particle samples through adjusting the sampling duration."

"TEM clearly shows the morphology of particles smaller than  $2\text{ }\mu\text{m}$ . For some larger particles,

we might further carry the scanning electron microscopy (SEM) experiments to determine their morphology. In this study, we did observe one fungi (*Yeast*) and one bacteria (*colibacillus*) sample through TEM, which were prepared in biological laboratories (Figure S2). Microscopic observations from the bacteria and fungi samples prepared in the laboratory were helpful to classify PBAPs emitted from the forest.

Once we clearly obtained electron images of different particles, we could then measure particle size and shape factors. In this study, the area, perimeter, shape factor, and equivalent circle diameter (ECD) of individual particles in TEM images are manually or automatically obtained through an image analysis software (RADUS, EMSIS GmbH, Germany). Based on these measurements, we can classify particle types and determine the diameter and shape factor of individual particles among different particle types. Moreover, we statistically analyze the number fractions in different size bins.”

3) I would also have liked to have seen a short section examining any meteorological influence and perhaps some short scale back trajectory analysis to attempt to define source regions.

Response: We added the back trajectories of air mass (Figure 1). Figure S1 listed the meteorological data during the sampling period.

## **New section 2.5 “Meteorological data and back trajectories**

### **“Meteorological data and back trajectories**

Meteorological data, including the relative humidity (RH), temperature, wind speed, and wind direction, were measured and recorded every 5 min by an automated weather meter (Kestrel 5500, USA). During the sampling period, the relative humidity (RH) and temperature varied from 40-70% and 22-28 °C during the day and 90-100% and 10-15 °C during the night, respectively. The wind speed was 1.5-7.6 m s<sup>-1</sup> during the day and 0-1 m s<sup>-1</sup> at night (Figure S4).

To determine the regional transport of air masses, 6-h back trajectories of air masses were generated using a Hybrid Single Particle Lagrangian Integrated Trajectory (HYSPLIT) model at the forest sampling station during 14-21 August, 2016. Based on the sampling times of each day at 09:00, 15:00, 21:00, and 02:00 (midnight) local time, we performed 31 air mass back trajectories. Here we selected an altitude of 500 m as the end point of each back trajectory (Figure 1). Figure 1 shows that all the back trajectories in the past 6-h had been transported over the Lesser Khingan Mountain forest.

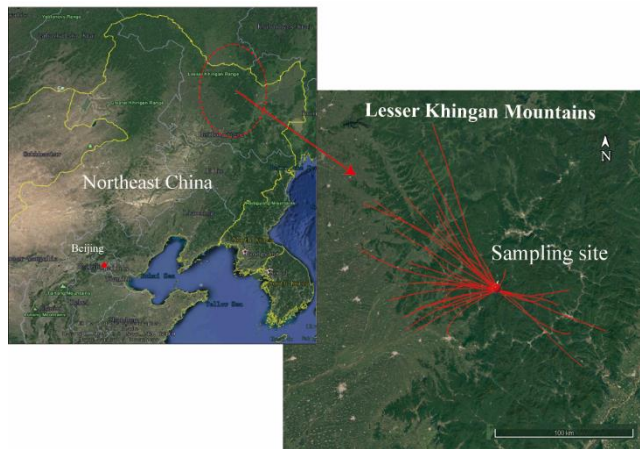


**Figure 1** Location of the sampling site and 6-h air mass back trajectories arriving at each sampling time from 14-21 August, 2016 in a boreal forest of the Lesser Khingan Mountain in Northeast China. The map source is Google Earth.

4) L65: Please be cautious of overinterpreting these results. A major criticism of these findings is that it is not possible to separate nucleation processes from scavenging, which should be noted. You may also wish to mention the bioprecipitation hypothesis in this section too, e.g., Morris et al., (2014).

Response: We thank the referee's comments here. We add the possible pathway and reference here. Here we cite this paper Morris et al., (2016), Bioprecipitation: a feedback cycle linking earth history, ecosystem dynamics and land use through biological ice nucleators in the atmosphere. *Glob Chang Biol*, doi: 10.1111/gcb.12447

The sentence was changed to P70-72 “These studies addressed the hypothesis that PBAPs indeed influence the hydrological cycle and climate by initiating the formation of clouds and precipitation as CCN and IN or the bioprecipitation feedbacks.”

5) L105: Whitehead et al., (2016) demonstrated up to 90% of detected particles at a Brasilian rainforest site to be PBAP, and likely fungal spores. They also demonstrated a strong, RH driven, diurnal variation in PBAP, which is consistent with arguments you make later in the paper so I recommend citing this work here.

Response: Thanks to provide such useful paper. Of course we need to cite it.

Whitehead et al., (2016): Biogenic cloud nuclei in the central Amazon during the transition from wet to dry season, *Atmos. Chem. Phys.*, 16, 9727-9743, <https://doi.org/10.5194/acp-16-9727-2016>

We also revised the part about the RH and PBAPs concentration and added the reference here. P465-471 “A similar phenomenon has been observed in different forests, such as the Amazon rainforest (Huffman et al., 2012; Whitehead et al., 2016), a montane ponderosa pine forest in North American (Crawford et al., 2014), a semi-arid forest in the southern Rocky Mountains of Colorado (Gosselin et al., 2016), and a semi-rural site in southwestern Germany (Toprak and Schnaiter, 2013). These studies above found that a nighttime peak of number concentrations of fluorescent

biological aerosol particles is consistent with nocturnal sporulation driven by the increased RH.”

6) L119: Please include the altitude of the site.

Response: Added the altitude here

Sentence revised: P125-127 “The sampling site is at the Heilongjiang Liangshui National Nature Reserve (47.32° N, 128.54° E; 350m above sea level) in the center of the Lesser Khingan Mountains of northeast China (Figure 1).”

7) L123: Please state the start and end time and dates of sampling.

Response: Added

Sentence changed to p130 “Because there is less rain in late August, we selected 14-21 August, 2016 to collect the bioaerosol samples.”

P137“We collected individual particles four times each day at 9:00, 15:00, 21:00, and 02:00 local time.”

8) L139: Please include a description of the sample handling procedure, including any steps taken to minimise contamination, e.g., as in Smith et al., (2018). Were substrate holders and the impactor assembly sterilised in any way prior to sampling? If so, how and with what frequency? I appreciate that you are not performing DNA extraction analysis or any other methods that require strict handling/contamination protocols in this study, but I feel it is a significant weakness to not include this information as it is needed to assess the reliability of your results. Have attempts been made to screen out biological particles introduced by contamination? If so can you quantify the amount of contamination?

Response: We appreciated that the referee carefully provided the reference here. In our experiment, the commercial TEM grids are made in superclean room in a company. The carbon film must be very clean and smooth before we use it. The silicon wafers are also made in superclean room in a company. It should be noted that the silicon wafers are covered by the plastic film to protect the smooth surface. Before we use it, we take the film off. Therefore, the substrates are no possible contamination. The holders and impactor are cleaned using alcohol before and after we use them in the field campaign.

We made one Figure in supplemental Figure S2 to explain our substrate and samplers. We added more steps to explain how to collect and storage the samples. In this study, because we didn't performing DNA extraction analysis, we only observe the particles on the substrate. Therefore, we only need to make sure the clean substrate before we used the substrate. Also, we need to make sure the storage condition in dry and sealed capsule. There is no possible to contact the contamination between sample and air. Also, in the condition, there is no condition for bacteria growth or other activity. In each field campaign, we prepared one blank sample as the background filter. The procedure might quantify the amount of contamination using the background filter through the same procedure. After we check the blank substrate, we didn't found any bacterial particles or fungus on the TEM grid and silicon wafer. Therefore, we can guarantee there is no contamination in the storage conditions. Based on two referee's comments, we further did the standard samples under the same procedure. The storage of PBAPs samples is no problem to obtain morphology of individual PBAPs.

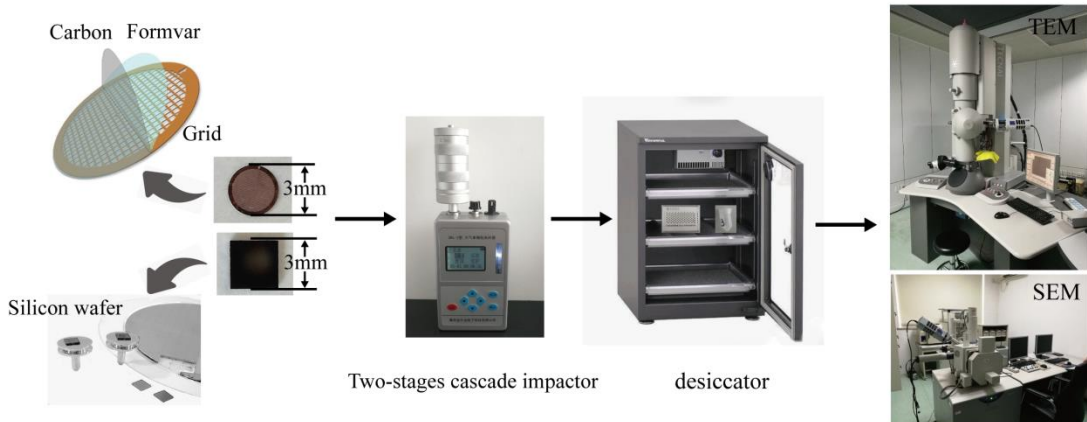


**Figure S1** The sampling procedures of substrate, sampler, storage, and analyzed technique.

9) L202: Here you state that more PBAP were observed at night than during the day. This is not a particularly novel result so I would ask the authors to include some citations to previous studies to contextualise this. Strong, RH driven, diurnal variation in PBAP concentrations at forest sites has previously been demonstrated by Crawford et al., (2014,2015), Gosselin et al., (2016), Toprak and Schnaiter (2013) & Whitehead et al., (2016) for example.

Response: We appreciated the referee to provide such good references. All of them were cited in section 3.2 in the revised manuscript.

P465-471“A similar phenomenon has been observed in different forests, such as the Amazon rainforest (Huffman et al., 2012;Whitehead et al., 2016), a montane ponderosa pine forest in North American (Crawford et al., 2014), a semi-arid forest in the southern Rocky Mountains of Colorado (Gosselin et al., 2016), and a semi-rural site in southwestern Germany (Toprak and Schnaiter, 2013). These studies above found that a nighttime peak of number concentrations of fluorescent biological aerosol particles is consistent with nocturnal sporulation driven by the increased RH.”

10) L202/Fig.3: I would like to see some of the data from the images tabulated here. Would it be possible to provide statistics of the particle size and aspect ratio for each of the PBAP types observed?

Response: Sure, we measured the data about the statistic of the particle size and aspect ratio of the PBAPs.

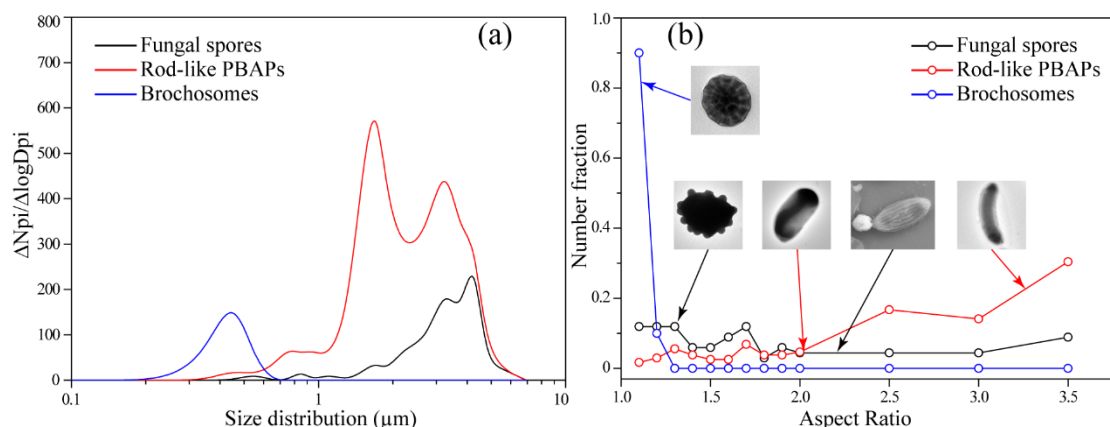


**Figure 6** Size distribution and aspect ratios of rod-like PBAPs, fungal spores, and brochosomes

collected in boreal forest air.

11) L210: Can you comment on the possibility of particle misclassification and how this is handled in subsequent analysis.

**Response:** As the two referee's comments about the classification, we did laboratory experiments to confirm the bacteria and fungi. Indeed, it is difficult to identify them based on their morphology from the electron microscopy. In the revised manuscript, we named "rod-like PBAPs" which contain bacteria and fungi. Besides the fine particles, TEM and SEM can clearly classify fungal spores and brochosomes due to their unique morphology. These two types of PBAPs have been well documented by SEM in many previous studies.

In the revised manuscript, we did more investigations from the literature and communicate more experts who concern the biological molecule, ecology, and bacteria. As the reason, we did additional laboratory experiments to confirm our classification. We believed that the revised classification can precisely deliver the right message for the potential readers.

12) L211: Can you please comment on how the inlet system used may have impacted your ability to detect pollen? If the inlet was fitted with a PM10 head then it would be expected that the majority of pollen would be too large to be sampled.

**Response:** The inlet is no problem to collect the large particles if pollens do exist in air. We collected coarse particles in desert and ocean air to study dust and sea salt particles before (Chi et al., ACP, 2015; Li et al., JGR, 2013). As the editor's suggestion, we did search more literature. Indeed, there was no pollen in August in boreal forest (Manninen et al., 2014).

In context p269 "Pollen was not found in our samples, which may be because large pollen emissions occur in spring and early summer instead of late summer (August) in boreal forests (Manninen et al., 2014)."

13) L296: Please contextualise this with other results in the literature as suggested earlier.

**Response:** Thanks. We carefully revised the part.

14) L298: A short section here examining the influence of other meteorological factors (e.g., wind speed/direction) and possibly short time scale back trajectory analysis would strengthen the paper as this would be useful to attempt to define source regions. Are higher counts observed at higher wind speeds or from specific wind sectors for example?

**Response:** Thanks. We added the back trajectories into the map. The wind speeds were shown in Figure S2. We also made discussion here about the wind speed.

In context p444-459 "It is well documented that meteorological conditions such as RH, wind speed, and temperature can affect PBAPs emission in the forests (Harrison et al., 2005; Whitehead et al., 2016). In particular, the wind speed is especially important in promoting PBAPs emission into air. During the sampling period, the average wind speeds at 5 min intervals had a range from 0 to 7.5 m/s with a mean value of 0.75 m/s. 89% of the measured wind speeds were lower than 2 m/s (Figure S4). Therefore, we conclude that no large consistent wind speeds occurred during the sampling period. Furthermore, we compared all the air mass back trajectories in the past 6-h over the Lesser Khingan Mountain forest at each sampling time (Figure 1). There are similar

lengths of these back trajectories, suggesting that wind speeds above the forest canopy had only small changes during the sampling period. Therefore, the result from the ground-based measurements of wind speeds is consistent with air mass back trajectories. Here, we can exclude wind speeds during the sampling period as one important factor to dominate PBAPs emissions during day and night in the boreal forest. High temperatures normally increase the PBAPs emissions from the plants in the daytime (Harrison et al., 2005). However, we observed contrasting results that more PBAPs occurred in nighttime instead of daytime (Figure S4). Therefore, we also exclude temperatures during the sampling period as a cause of the vastly different PBAPs emissions at day and night in the boreal forest.

”

15) L38/L352: I feel that the term full database overstates the work presented here as the particles are only broadly sub-classified and only a few select parameters are presented. Please scale this back. For me, a full database would require deeper classification with comprehensive statistics presented for each phyla or species as appropriate, which is lacking here.

**Response:** We noticed that we overstated it. We agreed with the referee's comments: The full database might include deeper classification with comprehensive statistics of each phyla or species. Here for electron microscopes, it is impossible to provide any species of PBAPs. Therefore, we deleted such words and made suitable tone here.

16) L45: Too general. Please rephrase. E.g., "At this boreal forest site: : :."

**Response:** Revised

17) L139: "a diameter of..."

**Response:** Revised

18) L233/Fig. 6: I'm not sure that bubble is the correct term. Suggest protrusion or protuberance.

**Response:** Revised

19) L369: Rephrase this sentence as it doesn't make sense as it is written. It may need splitting into two or more sentences. Fig.3: Define day and night in the caption.

**Response:** Revised

## References

Crawford et al., (2014): Characterisation of bioaerosol emissions from a Colorado pine forest: results from the BEACHON-RoMBAS experiment, *Atmos. Chem. Phys.*, 14, 8559-8578, <https://doi.org/10.5194/acp-14-8559-2014>

Crawford et al., (2015): Evaluation of hierarchical agglomerative cluster analysis methods for discrimination of primary biological aerosol, *Atmos. Meas. Tech.*, 8, 4979-4991, <https://doi.org/10.5194/amt-8-4979-2015>

Gosselin et al., (2016): Fluorescent bioaerosol particle, molecular tracer, and fungal spore

concentrations during dry and rainy periods in a semi-arid forest, *Atmos. Chem. Phys.*, 16, 15165-15184, <https://doi.org/10.5194/acp-16-15165-2016>

Morris et al., (2016), Bioprecipitation: a feedback cycle linking earth history, ecosystem dynamics and land use through biological ice nucleators in the atmosphere. *Glob Chang Biol*, doi: 10.1111/gcb.12447

Smith et al., (2018), Airborne Bacteria in Earth's Lower Stratosphere Resemble Taxa Detected in the Troposphere: Results From a New NASA Aircraft Bioaerosol Collector (ABC), *Front. Microbiol.*, doi:10.3389/fmicb.2018.01752

Toprak and Schnaiter (2013).: Fluorescent biological aerosol particles measured with the Waveband Integrated Bioaerosol Sensor WIBS-4: laboratory tests combined with a one year field study, *Atmos. Chem. Phys.*, 13, 225-243, <https://doi.org/10.5194/acp-13-225-2013>

Whitehead et al., (2016): Biogenic cloud nuclei in the central Amazon during the transition from wet to dry season, *Atmos. Chem. Phys.*, 16, 9727-9743, <https://doi.org/10.5194/acp-16-9727-2016>

1    **Overview of primary biological aerosol particles from a Chinese**  
2    **boreal forest: insight into morphology, size, and mixing state at**  
3    **microscopic scale**

4    Weijun Li<sup>1</sup>, Lei Liu<sup>1</sup>, Qi Yuan<sup>1</sup>, Liang Xu<sup>1</sup>, Yanhong Zhu<sup>1</sup>, Bingbing Wang<sup>2</sup>, Hua Yu<sup>3</sup>, Xiaokun  
5    Ding<sup>4</sup>, Jian Zhang<sup>1</sup>, Dao Huang<sup>1</sup>, Dantong Liu<sup>1</sup>, Wei Hu<sup>5</sup>, Daizhou Zhang<sup>6</sup>, Pingqing Fu<sup>5</sup>, Maosheng  
6    Yao<sup>7</sup>, Min Hu<sup>7</sup>, Xiaoye Zhang<sup>8</sup>, Zongbo Shi<sup>9,5</sup>

7    <sup>1</sup>Department of Atmospheric Sciences, School of Earth Sciences, Zhejiang University, Hangzhou  
8    310027, China

9    <sup>2</sup>State Key Laboratory of Marine Environmental Science, College of Ocean and Earth Sciences,  
10   Xiamen University, Xiamen 361102, China.

11   <sup>3</sup>College of Life and Environmental Sciences, Hangzhou Normal University, 310036, Hangzhou, China

12   <sup>4</sup>Department of Chemistry, Zhejiang University, Hangzhou 310027, China

13   <sup>5</sup>Institute of Surface-Earth System Science, Tianjin University, 300072, Tianjin, China

14   <sup>6</sup>Faculty of Environmental and Symbiotic Sciences, Prefectural University of Kumamoto,  
15   Kumamoto 862-8502, Japan

16   <sup>7</sup>State Key Joint Laboratory of Environmental Simulation and Pollution Control, College of  
17   Environmental Sciences and Engineering, Peking University, Beijing 100871, China

18   <sup>8</sup>Key Laboratory of Atmospheric Chemistry, Chinese Academy of Meteorological Sciences, Beijing,  
19   China

20   <sup>9</sup>School of Geography, Earth and Environmental Sciences, University of Birmingham, Birmingham  
21   B15 2TT, UK

22   \*Correspondence to: Weijun Li (liweijun@zju.edu.cn)

23 **Abstract:**

24 Biological aerosols play an important role in atmospheric chemistry, clouds, climate, and public  
25 health. Here, we studied the morphology and composition of primary biological aerosol particles  
26 (PBAPs) collected in the Lesser Khingan Mountain boreal forest of China in summertime using  
27 transmission electron microscopy (TEM) and scanning electron microscopy (SEM). C, N, O, P, K,  
28 and Si were detected in most of the PBAPs, and P represented a major marker to discriminate the  
29 PBAPs and non-PBAPs. Of all detected particles  $> 100$  nm in diameter, 13% by number were  
30 identified as PBAPs. We found that one type of PBAPs mostly appeared as similar rod-like shapes  
31 with an aspect ratio  $> 1.5$  and the dominant sizes ranged from 1  $\mu\text{m}$  to 5  $\mu\text{m}$ . The size distribution  
32 of the rod-like PBAPs displays two typical peaks at 1.4  $\mu\text{m}$  and 3.5  $\mu\text{m}$ , which likely are bacteria  
33 and fungal particles in the forest air. The second most PBAPs were identified as fungal spores with  
34 ovoid, sub-globular or elongated shapes with a smooth surface and small protuberances with their  
35 dominant size range of 2 - 5  $\mu\text{m}$ . Moreover, we found some large brochosomal clusters containing  
36 hundreds of brochosomes with a size range of 200-700 nm and a shape like a truncated icosahedron.  
37 The number size distribution of PBAPs coupled with  $\text{PM}_{2.5}$  and  $\text{PM}_{10}$  concentrations were used to  
38 estimate the total mass concentration of PBAPs, which is approximately 1.9  $\mu\text{g m}^{-3}$  and accounts  
39 for 47% of the in situ  $\text{PM}_{2.5-10}$  mass. Moreover, there is a higher frequency and concentration of  
40 PBAPs at night compared with day, suggesting that the relative humidity dramatically enhances the  
41 PBAPs emissions in the boreal forest. Our study also showed that the fresh PBAPs displayed weak  
42 hygroscopicity with a growth factor of  $\sim 1.09$  at RH=94%. TEM revealed that about 20% of the rod-  
43 like PBAPs were internally mixed with metal, mineral dust, and inorganic salts in the boreal forest  
44 air. This work for the first time provides the overview of individual PBAPs from nanoscale to  
45 microscale in Chinese boreal forest air.

46

47

48 **Key points**

49

50 • Based on morphology, composition, and size of individual PBAPs, rod-like PBAPs (e.g.,  
51 bacteria and fungi), fungal spores, and brochosomes were identified.

52 • PBAPs emissions tend to occur with high humidity at night rather than during the day.

53 • Hygroscopic experiments show that most of the PBAPs displayed weak hygroscopicity, and  
54 their growth factor was ~1.09 at RH=94%.

55

56 **1. Introduction**

57 Primary biological aerosol particles (PBAPs) (e.g., bacteria, spores, fungi, viruses, algae, and  
58 pollen) are ubiquitous in the Earth's atmosphere and **important** elements in the life cycle of many  
59 organisms and ecosystems (Poschl, 2005; Tunved et al., 2006; Smith et al., 2018). PBAPs are  
60 airborne biological materials that are transported from the biosphere to the atmosphere (Huffman et  
61 al., 2010), and they can account for a large proportion **(25-45%)** of the aerosol particle mass in  
62 pristine forest air **and certain amounts** in some rural and **marine air** (Elbert et al., 2007; Bauer et al.,  
63 2008; Hu et al., 2017; May et al., 2018). **The growing research** interest in **PBAPs** has one of its goals  
64 **to better understand how PBAPs or their** cell fragments **influence** cloud condensation nuclei (CCN)  
65 and ice nuclei (IN) (Morris et al., 2004; Huffman et al., 2013; Ling et al., 2018). Furthermore, field  
66 campaigns have found that abundant biological aerosols occur in cloud ice-crystals, fog/cloud, rain,  
67 and snowfall (Amato et al., 2005; Möhler et al., 2007; Christner et al., 2008; Pratt et al., 2009; Prenni  
68 et al., 2009; Tobo et al., 2013; Morris et al., 2014; Wilson et al., 2015; Twohy et al., 2016; Hu et al.,  
69 2018). These studies addressed the hypothesis that PBAPs indeed influence the hydrological cycle  
70 and climate by initiating the formation of clouds and precipitation as CCN and IN **or by their**  
71 **bioprecipitation feedbacks.**

72 Previous studies have investigated particle number concentration, size, and composition of  
73 primary biological aerosols using online measurement techniques and advanced molecular  
74 biological analyses (Wittmaack et al., 2005; Elbert et al., 2007; Fröhlich-Nowoisky et al.,  
75 2009; Huffman et al., 2010; Després et al., 2012; Crawford et al., 2015; Hu et al., 2017; Therkorn et  
76 al., 2017; Zhang et al., 2017; Chen and Yao, 2018). For example, the contribution of fungal spores to  
77 total organic carbon was estimated to be approximately 10% in clean and polluted periods in Beijing

78 using an online wideband integrated bioaerosol sensor (WIBS) (Yue et al., 2017); To obtain the  
79 organisms of PBAPs in the atmosphere, many studies tend to detect biochemical markers (e.g.,  
80 proteins, fatty acids, sugars) and nucleic acids (i.e., DNA and RNA) to determine their origins such  
81 as plant or animal debris, bacteria, fungi, or viruses (Georgakopoulos et al., 2009;Chen and Yao,  
82 2018;Hu et al., 2018;Ling et al., 2018). Although these previous studies provided comprehensive  
83 species or detailed molecular compositions of PBAPs, they still could not reflect the physical  
84 properties of individual PBAPs in the atmosphere, such as morphology, size, phase, hygroscopicity,  
85 and mixing state. Besides particle composition, the previous studies have proved that the  
86 morphology, size, and mixing state of individual particles more or less influence their CCN and IN  
87 activities and optical properties (Spracklen et al., 2008;Fröhlich-Nowoisky et al., 2009;Wilson et al.,  
88 2015;Li et al., 2016;Ault and Axson, 2017;Riemer et al., 2019). Therefore, it is critical to  
89 characterize detailed information of different types of individual PBAPs from their natural sources.

90 In the past decades, several studies have used scanning electron microscopy (SEM) to  
91 characterize the morphology and size of individual PBAPs (Nikkels et al., 1996;Wittmaack et al.,  
92 2005;Coz et al., 2010;Tamer Vestlund et al., 2014;Valsan et al., 2015;China et al., 2018). They  
93 identified fungal spores, brochosome, pollen, and plant or insect debris larger than 2  $\mu\text{m}$  in the  
94 atmosphere. Although the SEM observations adequately characterized the coarse fungal spores,  
95 pollen, and plant or insect debris particles, comparable results have not been obtained for fine  
96 bacteria and fungal particles, which together account for a large number of suspended particles in  
97 ambient air detected by online instruments (Tong and Lighthart, 2000;Després et al., 2012;Afanou  
98 et al., 2014;Valsan et al., 2016;Priyamvada et al., 2017;Hu et al., 2018). The reason for this shortfall  
99 is likely that SEM could not clearly observe carbonaceous bioaerosols smaller than 1  $\mu\text{m}$  (Li et al.,

100 2016;Ault and Axson, 2017). Posfai et al. (2003) and Patterson et al. (2016) used transmission  
101 electron microscopy (TEM) to detect some fine bacteria in marine air. However, there is no study  
102 to characterize the morphology, size, and mixing state of individual PBAPs from nanoscale to  
103 microscale. For example, many studies directly used SEM images showing the coarse PBAPs (e.g.,  
104 fungal spores) in support of their conclusions, but missed large numbers of fine PBAPs (e.g.,  
105 bacteria) (Shi et al., 2003;Wittmaack et al., 2005;Coz et al., 2009;Shi et al., 2009;Martin et al.,  
106 2010;Huffman et al., 2012;Tamer Vestlund et al., 2014;Afanou et al., 2015;Valsan et al.,  
107 2015;Valsan et al., 2016;Priyamvada et al., 2017;Wu et al., 2019). The result might discourage  
108 people considering fine bacteria and fungal particles for their atmospheric effects or for their  
109 examination of data from some online instruments. Therefore, it is necessary to integrate SEM and  
110 TEM to characterize the morphology, size, and mixing state of individual PBAPs from nanoscale to  
111 microscale.

112 Forests are important contributors of primary biological aerosols in the atmosphere (Tunved et  
113 al., 2006;Spracklen et al., 2008;Després et al., 2012;Whitehead et al., 2016). Aerosols in large  
114 forests contain abundant biological particles from plants emitted locally and lesser amounts of  
115 anthropogenic pollutants from long-range transport (Tong and Lighthart, 2000;Tunved et al.,  
116 2006;Gabey et al., 2010;Martin et al., 2010). We chose the Lesser Khingan Mountains in northeast  
117 China, which is its second largest boreal forest. In this study, TEM and SEM both have been  
118 employed to characterize the morphology, size, and mixing state of various PBAPs collected over  
119 the boreal forest. Furthermore, hygroscopic experiments on the primary biological particles have  
120 been conducted.

121

122 **2. Methods**

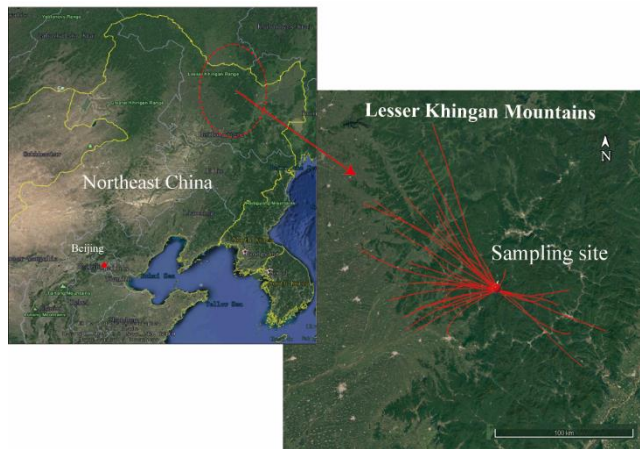
123 **2.1 Sampling site and sample collection**

124 The sampling site is at the Heilongjiang Liangshui National Nature Reserve (47.32°N, 128.54°  
125 E; 350m above sea level) in the center of the Lesser Khingan Mountains of northeast China (Figure  
126 1). The boreal region is characterized by large seasonal variations in temperature, and the flora is  
127 dominated by Korean pine and spruce species. There are no anthropogenic sources of pollutants,  
128 such as villages, industries and vehicles within 80 km of the sampling site. Boreal forests have the  
129 highest emissions of biological aerosols during summer. Because there is less rain in late August,  
130 we selected 14-21 August, 2016 to collect the bioaerosol samples.

131 Individual particle samples were collected both on copper (Cu) TEM grids coated with carbon  
132 film (carbon type-B, 300-mesh copper; Tianld Co., China) and on silicon membranes (thickness:  
133 500±10  $\mu$ m, size: 3×3 mm; LIJINGKEJI, China) by a single-stage cascade impactor called the DKL-  
134 2 sampler (Genstar Electronic Technology, China). The collection efficiency of the impactor is 50%  
135 for particles with an aerodynamic diameter of 0.1  $\mu$ m when we assume an aerosol particle density  
136 of 2 g cm<sup>-3</sup>. We collected individual particles four times each day at 9:00, 15:00, 21:00, and 02:00  
137 local time. At each sampling event, we first collected TEM grids and then changed to silicon wafers  
138 in the sampler. The sampling duration at each time varied from 10 min to 25 min depending on the  
139 particle distribution on the substrate. The substrates of the carbon film and silicon wafer both have  
140 smooth surfaces with no contamination before we use them to collect aerosol particles. After sample  
141 collection, we immediately performed optical microscopy (BST60-100, China) at 100X  
142 magnification to determine whether the aerosol distribution on the substrate was suitable for electron  
143 microscopy analysis. The distribution of aerosol particles on TEM grids was not uniform, with

144 coarser particles occurring near the center and finer particles on the periphery. The quick check by  
145 the optical microscopy enabled us to tell whether individual particles were well distributed and  
146 whether there was any overlap on the substrate. Whenever the distribution was not even enough or  
147 when substantial overlap occurred, we had to discard it and re-collect individual particle samples  
148 through adjusting the sampling duration. In a word, this sampling procedure guarantees that the  
149 collected particles were adequately separated and did not overlap each other on the substrate (Li et  
150 al., 2016). The Cu grids and silicon wafers were placed in a dry, clean, and airtight container with  
151 25 °C and 20±3% RH which minimizes exposure to ambient air and preserves them for subsequent  
152 analysis. The detailed sampling and storage procedures are summarized in Figure S1.

153 The daily PM<sub>2.5</sub> and PM<sub>10</sub> samples were collected on quartz-fiber filters with a diameter of 90  
154 mm through two medium-volume samplers (TH-150, Wuhan Tianhong, China) at a constant flow  
155 rate of 100 L min<sup>-1</sup>. The samples were changed at 08:00 a.m. each day. The DKL-2 and TH-150  
156 samplers and other monitoring instruments in the field experiment were installed on a building roof  
157 15 m above ground. The quartz filters (Whatman, UK) were put in polyethylene boxes immediately  
158 after sampling and stored at -5 °C. They were equilibrated at a constant temperature (20 ± 0.5 °C)  
159 and humidity (50 ± 2%) for over 24 h before being weighed with an electronic microbalance  
160 (Sartorius-ME5, Germany). This gravimetric procedure provides the mass concentration of PM<sub>2.5</sub>  
161 and PM<sub>10</sub>.



162

163 **Figure 1** Location of the sampling site and 6-h air mass back trajectories arriving at each  
 164 sampling time from 14-21 August, 2016 in a boreal forest of the Lesser Khingan Mountain in  
 165 Northeast China. The map source is Google Earth.

166 **2.2 Transmission electron microscopy analysis**

167 Individual aerosol particles collected on Cu grids were analyzed via transmission electron  
 168 microscopy (TEM, JEM-2100, JEOL Ltd., Japan) at a 200 kV accelerating voltage. TEM with a  
 169 beam of electrons is transmitted through a specimen to form an image. An image is formed from  
 170 the interaction of the electrons with the sample as the beam is transmitted through the specimen.  
 171 Therefore, TEM images display the inner physical structure of individual particles and the mixing  
 172 state of different components. The TEM system is equipped with an energy-dispersive X-ray  
 173 spectrometer (EDS, INCA X-Max<sup>N</sup> 80T, Oxford Instruments, UK). EDS is an analytical technique  
 174 used for the elemental analysis or chemical characterization of a sample. It relies on an interaction  
 175 between X-rays and a sample. EDS spectra show the peaks of different elements and the  
 176 contribution of each element in the total. EDS semiquantitatively detects the elemental composition  
 177 of individual particles with an atomic number greater than six ( $Z > 6$ ). However, Cu peaks in the  
 178 EDS spectra were not considered because of interference from the copper substrate of TEM grids.  
 179 We determined the morphology, composition, and mixing state of individual particles through the  
 180 combination of TEM and EDS. To reduce the damage to particles under the electron beam, the EDS  
 181 collection duration was limited to 15 s. Individual particles are distributed on TEM grids, with the  
 182 coarser particles in the center of sampling spot and with the finer particles on the periphery.  
 183 Therefore, to guarantee that the analyzed particles are representative, five areas are selected from

184 the sampling center to the periphery on each TEM grid. After a labor-intensive operation, we  
185 analyzed 150-250 individual particles with diameters of 100 nm-10  $\mu\text{m}$  in each sample. Finally, we  
186 successfully analyzed 20 TEM grids in the study. TEM/EDS can determine the internal mixing  
187 structure of different aerosol components in fine particles and their specific composition. TEM  
188 clearly shows the morphology of particles smaller than 2  $\mu\text{m}$ . For some larger particles, we might  
189 further carry the scanning electron microscopy (SEM) experiments to determine their morphology.  
190 In this study, we did observe one fungi (*Yeast*) and one bacteria (*colibacillus*) sample through TEM,  
191 which were prepared in biological laboratories (Figure S2). Microscopic observations from the  
192 bacteria and fungi samples prepared in the laboratory were helpful to classify PBAPs emitted from  
193 the forest.

194 Once we clearly obtained electron images of different particles, we could then measure particle  
195 size and shape factors. In this study, the area, perimeter, shape factor, and equivalent circle diameter  
196 (ECD) of individual particles in TEM images are manually or automatically obtained through an  
197 image analysis software (RADUS, EMSIS GmbH, Germany). Based on these measurements, we  
198 can classify particle types and determine the diameter and shape factor of individual particles among  
199 different particle types. Moreover, we statistically analyze the number fractions in different size bins.

200 Aspect Ratio is the maximum ratio between the length and width of a bounding box for the  
201 measured object. An aspect ratio of 1 (the lowest value) indicates that a particle is not elongated in  
202 any direction. The aspect ratio is defined as

$$203 \quad AR = \frac{L_{max}}{W_{max}}$$

204

### 205 2.3 Scanning electron microscopy analysis

206 SEM is performed using a type of electron microscope that can determine the particle surface  
207 by scanning it with a high-energy beam of electrons in a raster scan pattern. An SEM system (Zeiss  
208 Ultra 55) equipped with a field emission gun operating at 5–20 kV was used to obtain detailed  
209 information on the surfaces of individual aerosol particles. Moreover, the SEMx was equipped with  
210 an energy-dispersive X-ray spectrometry (EDS), which can analyze the chemical composition of

211 individual particles. The SEM/EDS can efficiently obtain the surface morphology, size, and  
212 composition of coarse particles without any coating process on the substrate. Finally, we selected  
213 six silicon wafers for SEM/EDS analysis (Figure S1). In this study, we used SEM/EDS to observe  
214 surface morphology of the coarse particles on silicon wafers and to confirm particle types which  
215 cannot be clearly shown in TEM images.

216 **2.4 Hygroscopic experiments**

217 A custom-made individual particle hygroscopic (IPH) system was used to observe the  
218 hygroscopic properties of individual biological particles at different relative humidity (RH)  
219 values (Figure 2). After the hygroscopic experiment, an SEM analysis of the sample was employed  
220 to primarily check particle types. This allowed us to further understand how PBAPs particles grow  
221 at different RH values ranging from 5% to 94%.

222 The scheme of the IPH system is shown in Figure 2, which consisted of four steps;  
223 (1) Introducing N<sub>2</sub> gas with a mass flow controller into a chamber;  
224 (2) Setting a TEM grid or silicon wafer on the bottom of an environmental microscopic cell  
225 (Gen-RH Mcell, UK), which can change the RH and maintain the temperature at 20 °C;  
226 (3) Taking images at incremental RH values using an optical microscope (Olympus BX51M,  
227 Japan) with a camera (Canon 650D);  
228 (4) Obtaining through the RADUS software the PBAPs sizes (i.e., D(RH) and D<sub>0</sub>) in the  
229 images taken from the optical microscopy manually or automatically.. The images can be taken  
230 at different RHs during hygroscopic experiments and then are input into the RADUS software  
231 for size measurement.

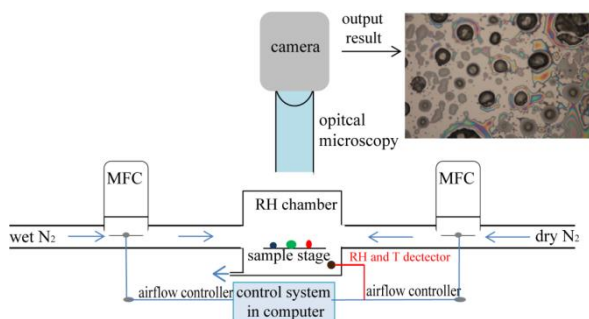
232 This IPH system has been tested and has successfully captured the hygroscopic growth of

233 individual aerosol particles collected on either a silicon wafer or TEM grid in our laboratory  
234 (Sun et al., 2018). Before the IPH system is used for ambient samples, it must be checked  
235 through standard NaCl particles on a silicon wafer made in the laboratory. Figure S3 shows that  
236 the delinquence relitive humidity (DRH) of individual NaCl particles on this silicon wafer is at  
237 76%, similar to the standard DRH at  $75 \pm 1\%$ . After the procedure, we can replace our collected  
238 samples into the IPH system.

239 The particle growth factor (GF), an important parameter used to describe the hygroscopic  
240 growth of individual particles, is defined as follows:

241 
$$GF(RH) = \frac{D(RH)}{D_0}$$

242 where  $D(RH)$  and  $D_0$  are the diameters of particles at a given RH and at 5% RH, respectively.



243  
244 **Figure 2** Scheme of a custom-made individual particle hygroscopic system to observe  
245 hygroscopic growth of individual particles

## 246

### 247 2.5 Meteorological data and back trajectories

248 Meteorological data, including the relative humidity (RH), temperature, wind speed, and  
249 wind direction, were measured and recorded every 5 min by an automated weather meter  
250 (Kestrel 5500, USA). During the sampling period, the relative humidity (RH) and temperature  
251 varied from 40-70% and 22-28 °C during the day and 90-100% and 10-15 °C during the night,

252 respectively. The wind speed was 1.5-7.6 m s<sup>-1</sup> during the day and 0-1 m s<sup>-1</sup> at night (Figure  
253 S4).

254 To determine the regional transport of air masses, 6-h back trajectories of air masses were  
255 generated using a Hybrid Single Particle Lagrangian Integrated Trajectory (HYSPLIT) model  
256 at the forest sampling station during 14-21 August, 2016. Based on the sampling times of each  
257 day at 09:00, 15:00, 21:00, and 02:00 (midnight) local time, we performed 31 air mass back  
258 trajectories. Here we selected an altitude of 500 m as the end point of each back trajectory  
259 (Figure 1). Figure 1 shows that all the back trajectories in the past 6-h had been transported  
260 over the Lesser Khingan Mountain forest.

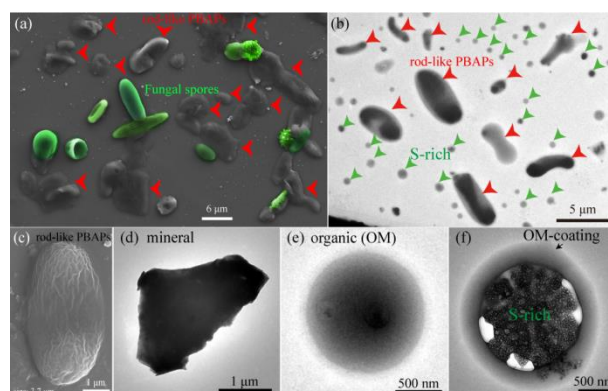
261 **3. Results and Discussion**

262 **3.1 Morphology and elemental composition of PBAPs**

263 Among the 4,122 analyzed aerosol particles with diameters of 100 nm-10  $\mu\text{m}$  analyzed by  
264 TEM/EDS, individual particles are classified into five groups based on their morphology and  
265 composition: S-OM (mixture of sulfate (S), organics (OM)), OM, mineral dust, and PBAPs (Figure  
266 3). S can be used to indicate secondary sulfates; abundant C and minor O with transparent color  
267 constitute the coating of the sulfate core and represent secondary organic matter; and irregular  
268 particles containing Si, Al, Ca, minor Fe, and Ti normally indicate mineral dust particles.  
269 Moreover, previous studies have found that elemental P in individual particles and their associated  
270 unique morphologies can be used to identify PBAPs by electron microscopy (Poschl,  
271 2005; Wittmaack et al., 2005). Thirteen percent of particles were PBAPs, and low magnification  
272 TEM and SEM images both revealed that abundant PBAPs occurred in the samples (e.g., Figure 3a-  
273 b).

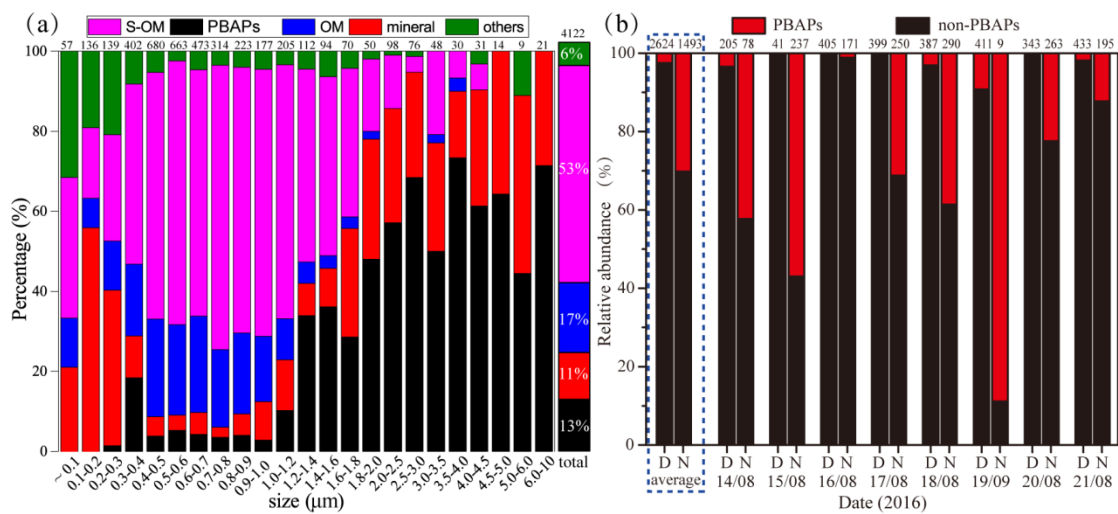
274 The number fractions of size-resolved aerosol particles show that secondary S-OM and OM  
275 particles were the dominant particle groups in the fine mode ( $< 1 \mu\text{m}$ ) while PBAPs and mineral  
276 particles dominated the coarse mode ( $\geq 1 \mu\text{m}$ ) (Figure 4a). Moreover, we noticed that the number  
277 fractions of PBAPs in each sample collected at night were much higher than those collected during  
278 the day. Abundant fine secondary sulfate and organic particles from photochemical formation were  
279 observed during the day. Figure 4b shows that the average number fraction of PBAPs was 2.5% in  
280 the samples collected during the day and as high as 30.0% at night. If we further calculated the  
281 number concentration of PBAPs in Figure 4b, the PBAPs concentration significantly increased by  
282 approximately seven times from daytime to nighttime, although the non-PBAPs concentration  
283 decreased.

284 Based on the morphology and size of the PBAPs, we definitely identified fungal spores and  
285 brochosomes, and plant or insect debris, all of which have been widely reported before (Wittmaack  
286 et al., 2005; Huffman et al., 2012; Afanou et al., 2014; Valsan et al., 2015; Priyamvada et al., 2017).  
287 Besides these PBAPs, we also found many special rod-like PBAPs with a dominant size range of 1  
288 - 5  $\mu\text{m}$ . Pollen was not found in our samples, which may be because large pollen emissions occur in  
289 spring and early summer instead of late summer (August) in boreal forests (Manninen et al., 2014).



291 **Figure 3** Low magnification SEM and TEM images of individual particles collected from the forest air.

292 (a) low magnification SEM image of rod-like PBAPs (red arrows) and fungal spores (green); (b) low  
 293 magnification TEM image of rod-like PBAPs particles and secondary sulfate (S-rich) particles; (c) SEM  
 294 image of a rod-like particle; (d) TEM image of a mineral dust particle (e) TEM image of an organic  
 295 matter (OM) particle; and (f) TEM image of OM coating on S-rich particles. The color in (a) was  
 296 artificially painted on the original SEM images.

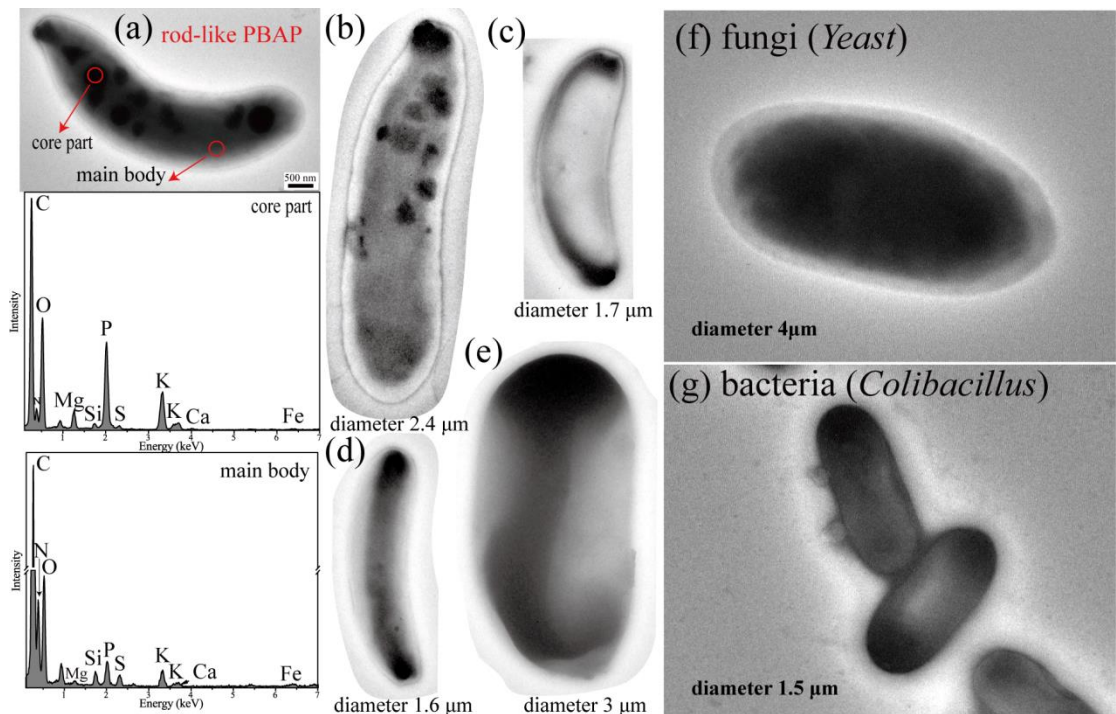


297 **Figure 4** Number fractions of different types of particles in different size bins and their total number  
 298 fraction (a); and number fractions of primary biological aerosol particles (PBAPs) and non-PBAPs  
 299 during the day and night (b). The number of analyzed particles is listed above each column. D and N are  
 300 daytime and nighttime.

302  
 303 Online instruments indicate that large number of fine PBAPs are bacteria and fungi in the forest  
 304 air (Tong and Lighthart, 2000; Elbert et al., 2007; Huffman et al., 2010; Després et al., 2012; Hu et al.,  
 305 2018). Although many previous studies reported PBAPs through the SEM, no observations of fine  
 306 bacteria and fungal particles in forest air were reported (Wittmaack et al., 2005; Shi et al.,  
 307 2009; Martin et al., 2010; Huffman et al., 2012; Tamer Vestlund et al., 2014; Valsan et al., 2015; Valsan  
 308 et al., 2016; Priyamvada et al., 2017; Wu et al., 2019). Posfai et al. (2003) found a few rod-like

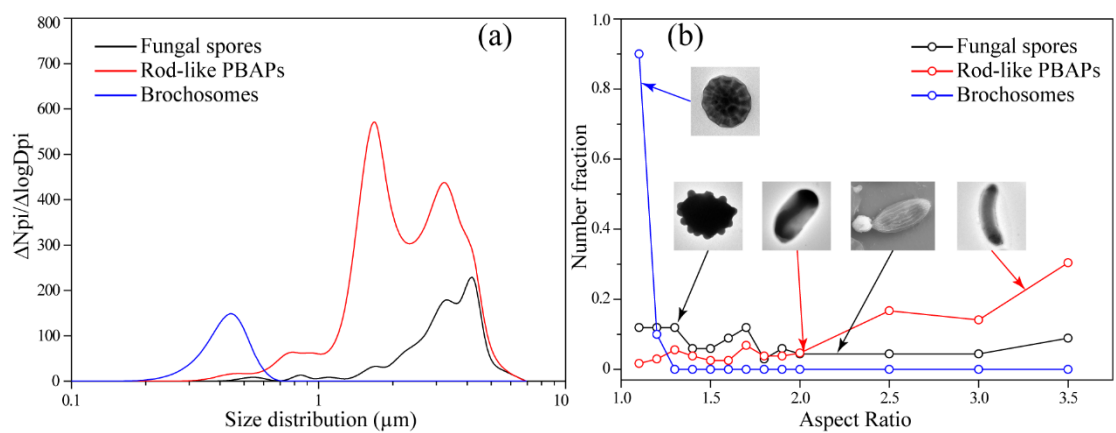
309 bacterial particles in marine air using TEM. In this study, we found that the rod-like PBAPs (Figure  
310 5a-e) have a morphology similar to bacteria reported by Posfai et al. (2003). These rod-like PBAPs  
311 were stable under the electron beam during the TEM analysis, and they contained C, N, O, P, and K  
312 with minor Mg, Si, S, Ca and Fe (Figure 5a). These rod-like PBAPs have a size range of 300 nm-7  
313  $\mu\text{m}$  with the dominant size range of 1-5  $\mu\text{m}$  with two typical peaks at 1.4  $\mu\text{m}$  and 3.5  $\mu\text{m}$  (Figure  
314 6a). Figure 6b further shows that the aspect ratio of 85% of these particles is larger than 1.5.

315 In nature, many fine fungi normally displayed similar composition and rod-like shape. To better  
316 compare and confirm differences of bacteria and fungi observed in TEM, we cultured *Colibacillus*  
317 and *Yeast* in the laboratory to represent bacteria and fungi. Then we sprayed the solution of  
318 *Colibacillus* and *Yeast* onto TEM grids. After drying these samples, we observed the morphology  
319 and size of *Colibacillus* and *Yeast* through the TEM (Figure 5f-g and Figure S5). Indeed, TEM/EDS  
320 show very similar rod-like shape and composition between *Colibacillus* and *Yeast* particles on the  
321 substrate, although the *Yeast* particles with a size range at 1-8  $\mu\text{m}$  with a mean diameter at 4.3  $\mu\text{m}$   
322 are larger than *Colibacillus* (300 nm-2.5  $\mu\text{m}$  with mean diameter of 1.3  $\mu\text{m}$ ) (Figure S5). It is  
323 interesting that the size distribution of the rod-like PBAPs collected in the forest air displays two  
324 typical peaks at 1.4  $\mu\text{m}$  and 3.5  $\mu\text{m}$ , which probably represent bacteria and fungi. Després et al.  
325 (2012) stated that bacteria mostly have diameters of 1-2  $\mu\text{m}$  and fungi of 1-10  $\mu\text{m}$  in the atmosphere.  
326 Although we can indicate the bacteria and fungi based on their sizes, the clue could not be used to  
327 precisely identify bacteria and fungi through electron microscopy due to their overlapped size range.  
328 Figure 6b shows 85% of particles with larger aspect ratios ( $> 1.5$ ), suggesting most of these PBAPs  
329 particles have typical rod-like shape. Although their identification is tentative, we called all these  
330 similar rod-like bacteria and fungal particles “rod-like PBAPs” here.



331

332 Figure 5 TEM image of the rod-like PBAPs collected in forest air and the fungi and bacteria  
 333 cultivated in laboratory. (a) Morphology of a rod-like PBAP and EDS spectra of its core and main  
 334 part. The red circles indicate where EDS impacted the rod-like PBAP. (b-e) Various rod-like PBAPs  
 335 collected in forest air. (f) One *Yeast* particle cultivated in laboratory (e) One *colibacillus* particle  
 336 cultivated in laboratory.



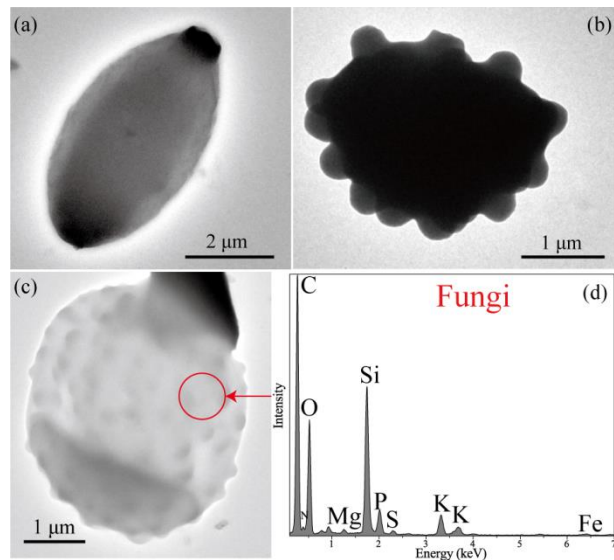
337

338 Figure 6 Size distribution and aspect ratios of rod-like PBAPs, fungal spores, and brochosomes  
 339 collected in boreal forest air.

340

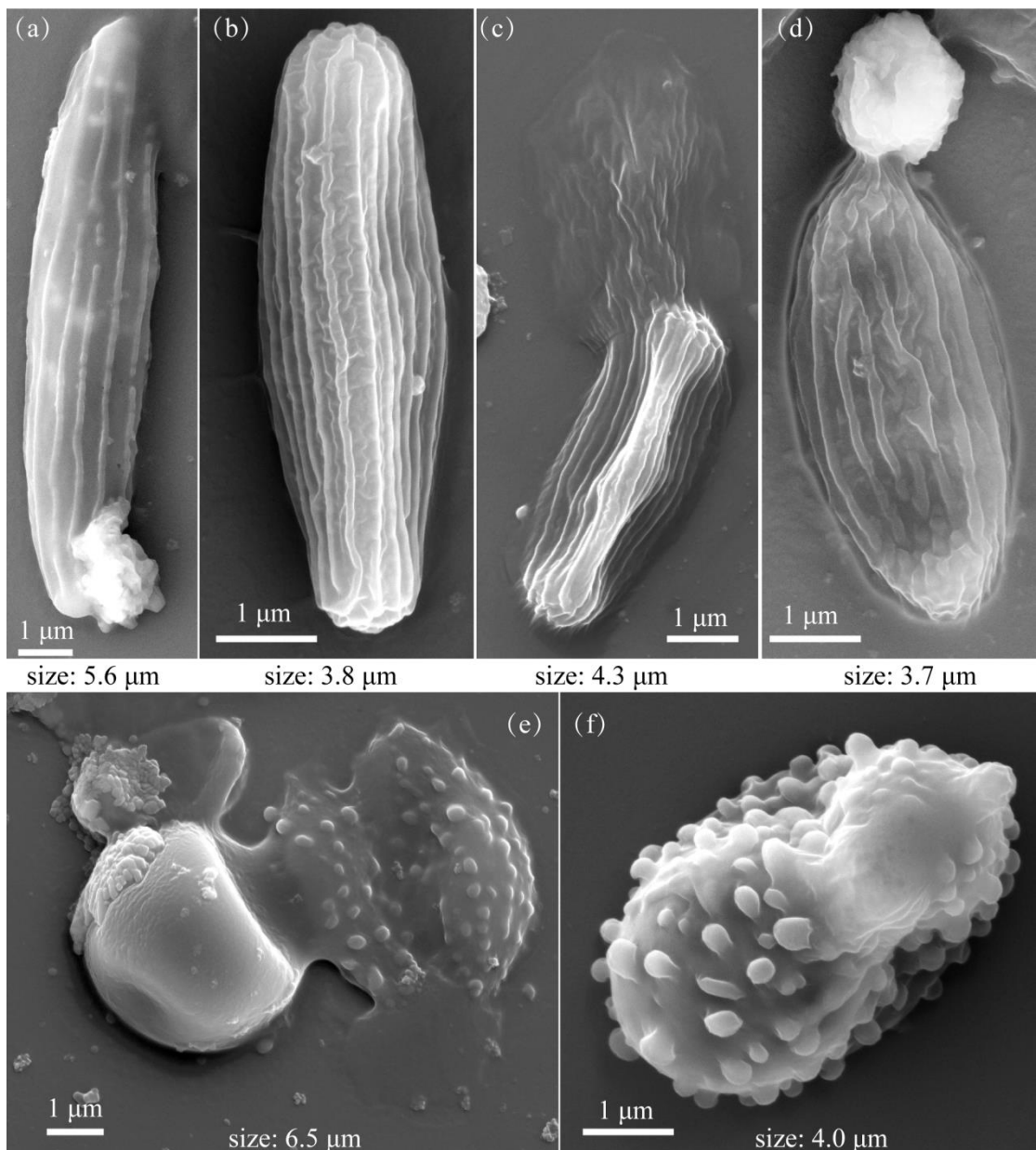
341 Fungal spores are microscopic biological particles that allow fungi to reproduce, serving a  
342 similar purpose to that of seeds in the plant world (Lacey and West, 2006). Spores can be released  
343 as a part of the sexual and/or asexual morph (stage) of the lifecycle of a fungus, and many species  
344 are able to produce spores from both stages (Després et al., 2012). Fungal spores have been reported  
345 in many places in the global air and their morphologies have been well documented (Shi et al.,  
346 2003;Wittmaack et al., 2005;Coz et al., 2009;Shi et al., 2009;Martin et al., 2010;Huffman et al.,  
347 2012;Tamer Vestlund et al., 2014;Afanou et al., 2015;Valsan et al., 2015;Valsan et al.,  
348 2016;Priyamvada et al., 2017;Wu et al., 2019). In this study, the fungal spores generally appeared  
349 as ovoid (Figure 7a), sub-globular (Figure 7b-c) or elongated shapes with a smooth surface and  
350 small protuberances (apiculus) (Figures 8a-f). Figure 7d shows that their composition mainly  
351 consists of C, O and Si, followed by minor N, Mg, P, S, K and Fe. The size range of the observed  
352 fungal spores varied roughly between 400 nm and 7  $\mu\text{m}$  (Figure 6a). The size distribution of fungal  
353 spores further showed a dominant size range of 2 - 5  $\mu\text{m}$  and one peak at 4  $\mu\text{m}$ . The number fraction  
354 of fungal spores at all aspect ratios is generally lower than 0.15, suggesting that there is no typical  
355 shape from either roundness or elongation for fungal spores in the boreal forest. SEM images clearly  
356 display that several typical fungal spores with diameters of 3.7-6.5  $\mu\text{m}$  do not have well-defined  
357 shapes and that their surfaces have regular strips or regular protuberances (Figure 8). Similar fungal  
358 spores have been reported in forest air (Wittmaack et al., 2005;Valsan et al., 2015). Compared with  
359 the rod-like PBAPs, fungal spores normally have a rougher surface (Figures 6-7), larger size, and  
360 much higher Si and lower N. Therefore, the fungal spores can easily be identified based on their  
361 morphology among the PBAPs through the TEM and SEM analysis.

362



363 **Figure 7** TEM/EDS showing the morphology and composition of various fungal spores. (a) a  
364 spindle fungal spore; (b) a fungal spore with protuberances; (c) a fungal spore with protuberances;  
365 and (d) EDS spectrum showing the composition of fungal spore. The red circle indicates where EDS  
366 impacted the particle.

367



368

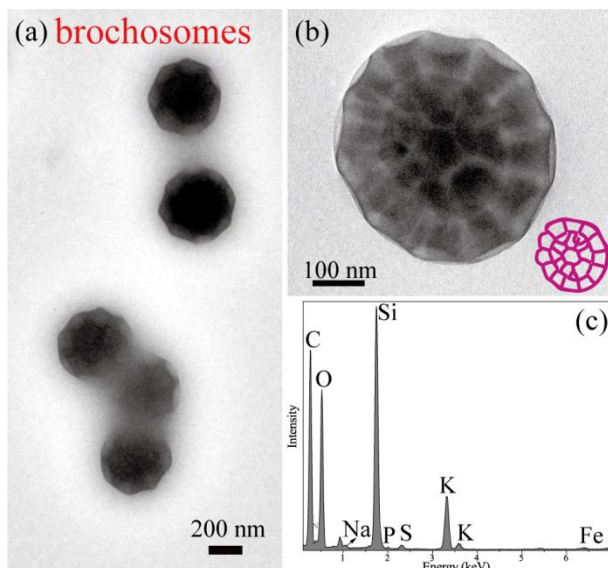
369 **Figure 8** SEM images showing the shape, size, and surface properties of fungal spores. Size  
 370 represents the diameter of fungal **spores**. (a-d) Surfaces of three **spindle** fungal particles with a layer  
 371 of strips. (e-f) Surfaces of two fungal **spores** with protuberances.

372

373 Brochosomes are hollow spherical particles produced by leafhoppers (Cicadelliae)  
 374 (Wittmaack, 2005). TEM and SEM observations both found abundant brochosomes in the samples.  
 375 The low-magnification SEM images showed that there are large brochosomal clusters on the  
 376 substrate, each containing tens or hundreds of single brochosomes (Figure S6). Wittmaack (2005)

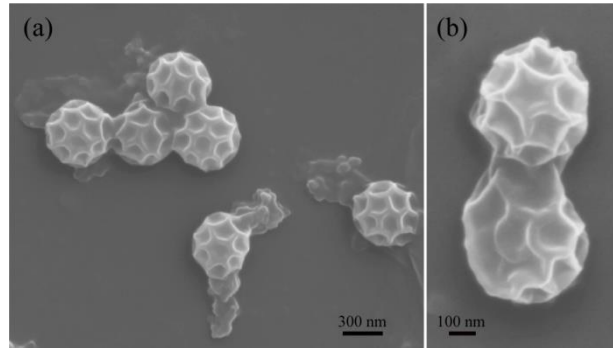
377 found that most of the brochosomes normally occur as large clusters and reported that each cluster  
378 contains up to 100,000 brochosomes. In this study, TEM and SEM both produce clear images  
379 showing the structure of the brochosome (Figures 9-10). Interestingly, the outline of each  
380 brochosome approximates a truncated icosahedron and the brochosome particles likely have unique  
381 inner structures, such as C60 Buckminster fullerenes (Figures 9a-b and 10). Compared with the rod-  
382 like PBAPs, chemical composition of the brochosomal particles show extremely high Si and low P  
383 in addition to major C and O and minor N, Na, S, K and Fe (Figure 9c). A single brochosome has a  
384 size range of 200-700 nm with a mean diameter of 350 nm. The aspect ratio of individual  
385 brochosomes is close to 1, suggesting that they are spherical (Figure 6b). Because the brochosomes  
386 might be dispersed from their clusters when they impact on the substrate, it is not meaningful to  
387 compare the number fraction of brochosomes with the rod-like PBAPs and fungal spores.

388



389 **Figure 9** TEM images of brochosomes and the composition of (a) a single brochosome and brochosome  
390 aggregations; (b) high-resolution TEM image showing the inner structure of one brochosome; (c) EDS  
391 spectrum showing the chemical composition of the brochosomes.

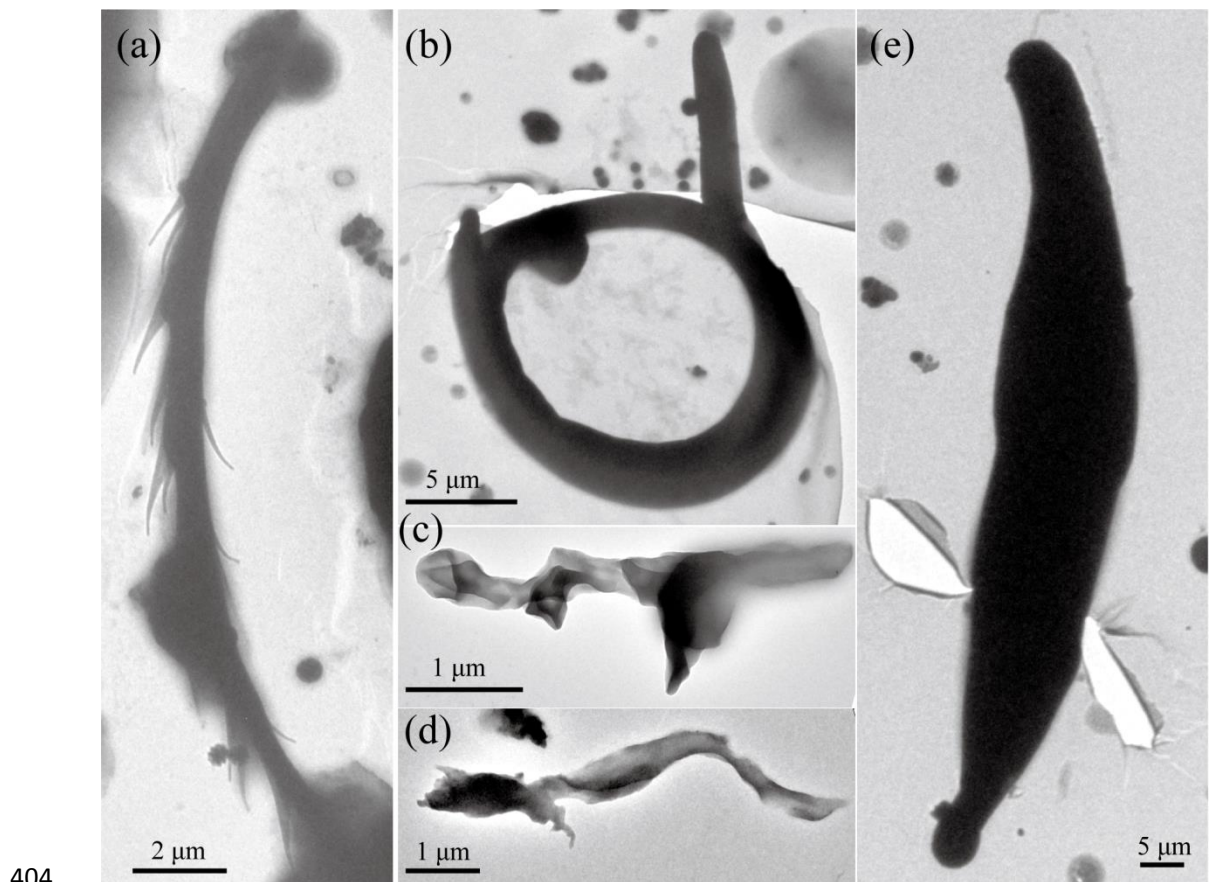
392



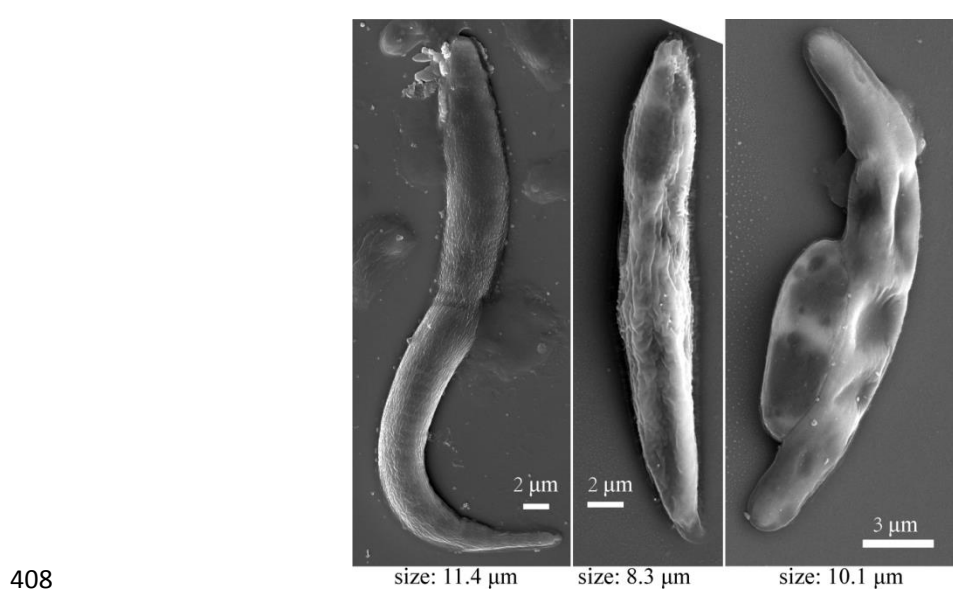
393 **Figure 10** SEM images of brochosomes. (a) Single brochosome and their aggregations. Some  
394 brochosomal particles are associated with primary biological species. (b) High-resolution SEM image  
395 showing the surface properties of the brochosomal particles.

396

397 The TEM and SEM images both show a few elongated large particles at 8-20  $\mu\text{m}$  among the  
398 biological particles. EDS shows that these particles mainly contained C, O, and Si but no detectable  
399 P in some of these biological particles as shown in Figures 11-12. We speculate that these biological  
400 particles were plant or insect debris. For example, Wittmaack et al. (2005) suggested that the  
401 spaghetti-type biological particles from Figure 11a-d are likely epicuticular wax fragments of plants.  
402 The SEM images as shown in Figure 12 clearly displayed the surface morphology of the large  
403 particles.



405 **Figure 11** TEM images showing the morphology of the primary biological particles. (a) One elongated  
 406 particle with thorns; (b) one circular particle; (c-d) two elongated particles; and (e) one long spindle  
 407 particle



409 **Figure 12** SEM image showing the morphology and surface properties of three elongated biological

410 particles.

411 **3.2 Relative abundance of PBAPs**

412 In this study, we classified PBAPs but also efficiently obtained the number fraction of rod-like  
413 PBAPs and fungal spores in coarse mode particles ( $> 1 \mu\text{m}$ ). The results from the electron  
414 microscopy analysis further estimated that PBAPs, mineral dust, and the remaining particles  
415 accounted for 50%, 25%, and 25% of the coarse mode, respectively. Assuming a density of  $\sim 1 \text{ g}$   
416  $\text{cm}^{-3}$  for PBAPs (Elbert et al., 2007),  $2 \text{ g cm}^{-3}$  for mineral dust particles, and  $1.4 \text{ g cm}^{-3}$  for the  
417 remaining particles (e.g., S-OM, OM, and metal) (Rissler et al., 2006), mass concentrations of the  
418 three different types of particles with different size bins can be estimated based on the equation:

419 
$$M_i = \frac{\pi}{6} D_i^3 \rho_i N_i$$

420  $i$ : particle type (PBAPs, mineral dust, and other remaining particle)

421 D: particle geometrical diameter in a size bin

422 N: particle number in a size bin

423 M: total mass of the analyzed particles in a size bin

424  $\rho$ : particle density ( $\text{g cm}^{-3}$ )

425 In the equation,  $N_i$  and  $D_i$  both can be obtained through the measurement of individual particles  
426 in TEM images. Finally, we estimated that the mass concentration of PBAPs, mineral dust, and  
427 remaining particles accounted for 47%, 43%, and 10% of  $\text{PM}_{2.5-10}$ , respectively. The results suggest  
428 that PBAPs significantly contributed to mass concentration of  $\text{PM}_{2.5-10}$  in summertime in the boreal  
429 forest air. During the sampling period, we measured the daily mass concentrations of  $\text{PM}_{2.5}$  of  $\sim 6.0$   
430  $\mu\text{g m}^{-3}$  and  $\text{PM}_{10}$  of  $\sim 10.0 \mu\text{g m}^{-3}$ . The number size distribution of PBAPs coupled with the mass  
431 concentrations of  $\text{PM}_{2.5}$  and  $\text{PM}_{10}$  were used to estimate the total mass concentration of PBAPs

432 using the result from the above equation. We estimated that the PBAPs contributed  $\sim 1.9 \mu\text{g m}^{-3}$  to  
433 the concentration of  $\text{PM}_{2.5-10}$  of  $4.0 \mu\text{g m}^{-3}$ .

434 Thirteen percent of all detected particles **by number** collected from the boreal forest air are  
435 PBAPs. Such a high fraction of PBAPs has not been reported in urban and rural air in China (Shi et  
436 al., 2003; Shi et al., 2009; Li et al., 2016). We noticed that the number concentration of PBAPs was  
437 much higher at night than during the day (Figure 3b). A shallow nocturnal boundary layer can lead  
438 to a **slight** increase in the number concentration of coarse particles near the ground (Graham et al.,  
439 2003), **but** this increase cannot explain the large difference in the relative number fraction of PBAPs  
440 (12 times larger at night than during the day) (Figure 3b). Alternately, the relative emission strength  
441 of PBAPs **from the forest between day and night likely induced the difference of the relative number**  
442 **fractions.**

443 It is well documented that meteorological conditions such as RH, wind speed, and temperature  
444 can affect PBAPs emission in the forests (Harrison et al., 2005; Whitehead et al., 2016). In particular,  
445 the wind speed is especially important in promoting PBAPs emission into air. During the sampling  
446 period, the average wind speeds at 5 min intervals had a range from 0 to 7.5 m/s with a mean value  
447 of 0.75 m/s. 89% of the measured wind speeds were lower than 2 m/s (Figure S4). Therefore, we  
448 conclude that no large consistent wind speeds occurred during the sampling period. Furthermore,  
449 we compared all the air mass back trajectories in the past 6-h over the Lesser Khingan Mountain  
450 forest at each sampling time (Figure 1). There are similar lengths of these back trajectories,  
451 suggesting that wind speeds above the forest canopy had only small changes during the sampling  
452 period. Therefore, the result from the ground-based measurements of wind speeds is consistent with  
453 air mass back trajectories. Here, we can exclude wind speeds during the sampling period as one

454 important factor to dominate PBAPs emissions during day and night in the boreal forest. High  
455 temperatures normally increase the PBAPs emissions from the plants in the daytime (Harrison et  
456 al., 2005). However, we observed contrasting results that more PBAPs occurred in nighttime instead  
457 of daytime (Figure S4). Therefore, we also exclude temperatures during the sampling period as a  
458 cause of the vastly different PBAPs emissions at day and night in the boreal forest.

459 Besides wind speed and temperature, RH is an important meteorological variable that  
460 influences PBAPs emissions from plants (Harrison et al., 2005; Huffman et al., 2012). In this study,  
461 we found large differences of RH between day and night (Figure S4). The elevated RH near 100%  
462 at night (Figure S1) appears to be an important factor that increases the emissions of PBAPs. This  
463 result is consistent with the conclusion of Elbert et al. (2007), who showed that PBAPs in a boreal  
464 forest are generally most abundant in samples collected at night when the RH is close to 100%. A  
465 similar phenomenon has been observed in different forests, such as the Amazon rainforest  
466 (Huffman et al., 2012; Whitehead et al., 2016), a montane ponderosa pine forest in North American  
467 (Crawford et al., 2014), a semi-arid forest in the southern Rocky Mountains of Colorado (Gosselin  
468 et al., 2016), and a semi-rural site in southwestern Germany (Toprak and Schnaiter, 2013). These  
469 studies above found that a nighttime peak of number concentrations of fluorescent biological aerosol  
470 particles is consistent with nocturnal sporulation driven by the increased RH. Moreover, Troutt and  
471 Levetin (2001) explained that the increase in PBAP concentrations is caused by the increase in  
472 basidiospores concentrations with RH, and they showed that a clear diurnal rhythm occurs and peaks  
473 at 04:00-06:00 LT. Furthermore, the number ratio (4.6 at nighttime and 4.0 at daytime) of rod-like  
474 PBAPs vs fungal spores and their number concentrations increased from daytime to nighttime  
475 (Figure S7). These results all suggest that higher RH can promote the emissions of rod-like PBAPs

476 and fungal spores in the boreal forest.

477

478 **3.3 Mixing state of rod-like PBAPs**

479 Our study shows that rod-like PBAPs contain bacteria and fungi in the boreal forest air.

480 Although approximately 80% of rod-like PBAPs were externally mixed particles in the boreal forest

481 air, we still found that 20% of rod-like PBAPs were internally mixed particles. TEM observations

482 show that the rod-like PBAPs were frequently internally mixed with mineral, metal, organics, and

483 inorganic salts. We noticed that irregular mineral dust particles significantly changed the shape of

484 the rod-like PBAPs (Figure 13a-c). The EDS analysis shows that the internally mixed mineral

485 particles contain certain amounts of C, O, and P in addition to Si, Al, or Ca (Figure 13a-c),

486 suggesting that many rod-like PBAPs were associated with mineral dust particles.

487 In this study, we found that some nanoscale metal particles were internally mixed with rod-like

488 PBAPs. Figure 13d-f further shows that these metals were spherical and contained Mn, Si and/or

489 Fe. As in previous studies, these nanosize metal particles were emitted from industrial activities or

490 power plants instead of natural soil (Li et al., 2017). TEM observations show that these metallic

491 particles were mainly attached to the surface of rod-like PBAPs. Moreover, some rod-like PBAPs

492 were coated by inorganic salts (e.g., K-P in Figure 13g and S-rich in Figure 13i) and organics. The

493 shape of the rod-like PBAPs might change following the aging process during long-range transport

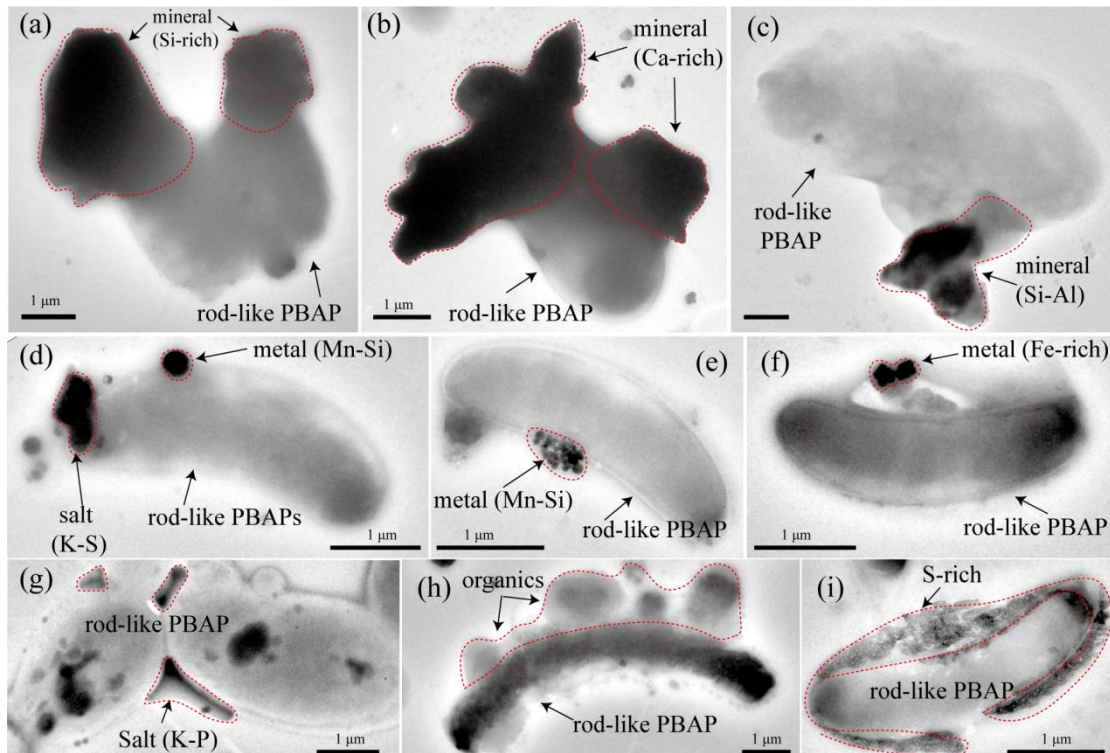
494 (Figure 13), although the elemental P or its associated ionic components ( $H_2PO_4^-$  and  $PO_3^-$ ) did not

495 change (Pratt et al., 2009). Pratt et al. (2009) detected  $H_2PO_4^-$  and  $PO_3^-$  in individual cloud ice-

496 crystal residues to identify PBAPs using aerosol time-of-flight mass spectrometry. Although one

497 study indicates that a few mineral dust or fly ash particles contain trace inorganic P, these particles

498 do not contain abundant organics and their number is low in the air (Zawadowicz et al., 2017).  
 499 Therefore, TEM/EDS is an efficient tool to identify fine bacteria or fungi from non-PBAPs collected  
 500 in the atmosphere. Moreover, it significantly reveals the mixing state of individual PBAPs, a key to  
 501 understand their possible CCN and IN activity over the boreal forest air in the future.



502 **Figure 13** TEM showing the internally mixed rod-like PBAPs. (a-c) Internal mixture of mineral and rod-  
 503 like PBAP; (d-f) Internal mixture of metal and rod-like PBAP; (g) Internal mixture of inorganic salts and  
 504 rod-like PBAP; (h) Internal mixture of organics and rod-like PBAP; and (i) Internal mixture of S-rich  
 505 salts and rod-like PBAP.

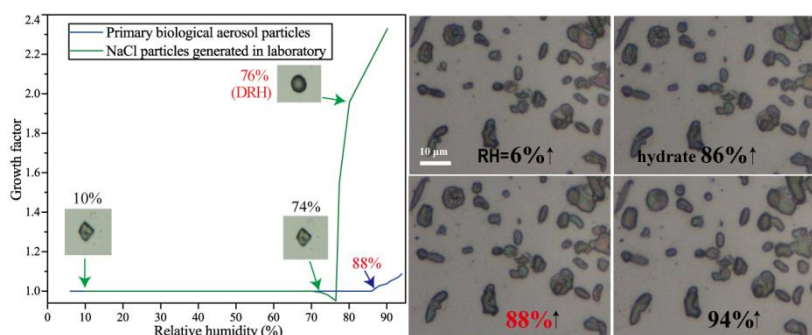
507

### 508 3.4 Hygroscopicity of PBAPs

509 In this study, we conducted an experiment to observe the hygroscopic growth of fresh PBAPs.  
 510 In the hygroscopic experiment, the PBAPs all take up water and grow by up to 88% during hydration,  
 511 and they lose water and return to the dry particle size (reduction of 83%) during dehydration (Figure

512 14). The growth factor of the PBAPs is ~1.09 at RH=94% based on the particle diameter change,  
513 which is much lower than growth factor of NaCl at ~2.3 (Figure 14). These results show that the  
514 fresh PBAPs have extremely weak hygroscopicity.

515 Recent studies found that fungal fragments collected in Amazon forests displayed strong  
516 hygroscopic properties (China et al., 2016;China et al., 2018) and were internally mixed with certain  
517 amounts of sodium salts. However, we found weak hygroscopic growth of 1.09, whereas this value  
518 was in the range of 1.05-1.3 for bacteria and fungal spores in previous studies (Reponen et al.,  
519 1996;Lee et al., 2002). However, the result is much lower than the value of 2.30 at RH=94% for  
520 NaCl (Figure 2a) and 1.60 at RH 94% for ammonium sulfate (Sun et al., 2018). This comparison  
521 suggests that fresh PBAPs display extremely weak hygroscopicity and do not contain any sodium  
522 salt in the boreal forest (Figure 2a). Overall, our results indicate that PBAPs from the substantial  
523 biological emissions from the Khingan Mountain boreal forest are weakly hygroscopic in nature.



524  
525 **Figure 14** Hygroscopic growth of NaCl prepared in laboratory and primary biological particles  
526 collected in boreal forest air. The up arrows (i.e., RH) represent hydration.

527

#### 528 **4. Conclusions**

529 The TEM and SEM observations both showed that the morphology of PBAPs were unique;  
530 they differed markedly from that of the sulfate, mineral, soot, organics, and metal particles in

531 continental air. Our results indicate that significant amounts of PBAPs are emitted from the Khingan  
532 Mountain area. In this study, we establish detailed information that includes the morphology, size,  
533 and composition of rod-like PBAPs, fungal spores, and brochosomes. C, N, O, P, K, and Si were  
534 detected in most of the PBAPs, and P represented a major marker to discriminate the PBAPs and  
535 non-PBAPs. We found that one type of PBAPs mostly appeared as similar rod-like shapes with an  
536 aspect ratio > 1.5 and the dominant sizes ranged from 1  $\mu\text{m}$  to 5  $\mu\text{m}$ . The size distribution of the  
537 rod-like PBAPs displays two typical peaks at 1.4  $\mu\text{m}$  and 3.5  $\mu\text{m}$ , which likely represent bacteria  
538 and fungal particles in the forest air. However, our study shows that there was no clear boundary  
539 between bacteria and some fungi from their size because of their size range partly overlapped.

540 The second most plentiful PBAPs were identified as fungal spores with ovoid, sub-globular or  
541 elongated shapes with a smooth surface and small protuberances (apiculus) with size at 400 nm - 7  
542  $\mu\text{m}$  with a mean diameter of 4  $\mu\text{m}$ . Moreover, we found some large brochosomal clusters containing  
543 hundreds of brochosomes which have sizes from 200-700 nm and shapes like truncated  
544 icosahedrons. We estimated that the mass concentration of PBAPs, mineral dust, and remaining  
545 particles accounted for 47%, 43%, and 10% of the PM<sub>2.5-10</sub> mass concentration, respectively,  
546 indicating that large boreal forests might represent a major source of PBAPs in the atmosphere.  
547 Moreover, there is a higher frequency and concentration of PBAPs at night compared with day. This  
548 difference could not be explained by wind speed or temperature, but was explicable by RH, which  
549 appears to be critical in enhancing PBAPs emissions from plants at night. The hygroscopic  
550 experiment shows that the primary bacterial and fungal particles show weak hygroscopicity.  
551

552 **Author Contributions:** WL designed the study. WL, LL, QY, LX, and HY collected  
553 aerosol particles. WL, QL, LL, LX, YZ, BW, XD, and JZ contributed laboratory  
554 experiments and data analysis. WL prepared the manuscript with contributions from  
555 all the coauthors. BW, DH, DL, WH, DZ, PF, MY, MH, XZ, and ZS commented and  
556 edited the paper.

557

558 **Competing interests:** The authors declare no competing financial interests

559

560 **Acknowledgments**

561 We appreciate Peter Hyde's comments and proofreading. **We appreciate Min Yue and Jiachang**  
562 **Lian (Zhejiang Univ.) providing the *Yeast* and *Colibacillus* cultures. Huijun Xie (Shandong**  
563 **Univ.) is thanked for discussions.** This work was funded by the National Natural Science  
564 Foundation of China (9184430003, 41622504 and 41575116), Zhejiang Provincial Natural  
565 Science Foundation of China (LZ19D050001), and Zhejiang University Education Foundation  
566 Global Partnership Fund. All the data are presented in the paper.

567

568

569 **References:**

570 Afanou, K. A., Straumfors, A., Skogstad, A., Nilsen, T., Synnes, O., Skaar, I., Hjeljord, L., Tronsmo, A.,  
571 Green, B. J., and Eduard, W.: Submicronic Fungal Bioaerosols: High-Resolution Microscopic  
572 Characterization and Quantification, *Appl. Environ. Microb.*, 80, 7122-7130, 10.1128/aem.01740-14,  
573 2014.

574 Afanou, K. A., Straumfors, A., Skogstad, A., Skaar, I., Hjeljord, L., Skare, Ø., Green, B. J., Tronsmo, A.,  
575 and Eduard, W.: Profile and Morphology of Fungal Aerosols Characterized by Field Emission Scanning  
576 Electron Microscopy (FESEM), *Aerosol Sci. and Tech.*, 49, 423-435, 10.1080/02786826.2015.1040486,  
577 2015.

578 Amato, P., Ménager, M., Sancelme, M., Laj, P., Mailhot, G., and Delort, A.-M.: Microbial population in  
579 cloud water at the Puy de Dôme: Implications for the chemistry of clouds, *Atmos. Environ.*, 39, 4143-  
580 4153, <https://doi.org/10.1016/j.atmosenv.2005.04.002>, 2005.

581 Ault, A. P., and Axson, J. L.: Atmospheric Aerosol Chemistry: Spectroscopic and Microscopic Advances,  
582 *Anal. Chem.*, 89, 430-452, 10.1021/acs.analchem.6b04670, 2017.

583 Bauer, H., Schueller, E., Weinke, G., Berger, A., Hitzenberger, R., Marr, I. L., and Puxbaum, H.:  
584 Significant contributions of fungal spores to the organic carbon and to the aerosol mass balance of the  
585 urban atmospheric aerosol, *Atmos. Environ.*, 42, 5542-5549,  
586 <https://doi.org/10.1016/j.atmosenv.2008.03.019>, 2008.

587 Chen, H., and Yao, M.: A high-flow portable biological aerosol trap (HighBioTrap) for rapid microbial  
588 detection, *J. Aerosol Sci.*, 117, 212-223, <https://doi.org/10.1016/j.jaerosci.2017.11.012>, 2018.

589 China, S., Wang, B., Weis, J., Rizzo, L., Brito, J., Cirino, G. G., Kovarik, L., Artaxo, P., Gilles, M. K.,  
590 and Laskin, A.: Rupturing of Biological Spores As a Source of Secondary Particles in Amazonia, *Environ.*  
591 *Sci. Technol.*, 50, 12179-12186, 10.1021/acs.est.6b02896, 2016.

592 China, S., Burrows, S. M., Wang, B., Harder, T. H., Weis, J., Tarhan, M., Rizzo, L. V., Brito, J., Cirino,  
593 G. G., Ma, P.-L., Cliff, J., Artaxo, P., Gilles, M. K., and Laskin, A.: Fungal spores as a source of sodium  
594 salt particles in the Amazon basin, *Nat. Commun.*, 9, 4793, 10.1038/s41467-018-07066-4, 2018.

595 Christner, B. C., Cai, R., Morris, C. E., McCarter, K. S., Foreman, C. M., Skidmore, M. L., Montross, S.  
596 N., and Sands, D. C.: Geographic, Seasonal, and Precipitation Chemistry Influence on the Abundance  
597 and Activity of Biological Ice Nucleators in Rain and Snow, *P. Natl. Acad. Sci.*, 105, 18854-18859, 2008.

598 Coz, E., Gómez-Moreno, F. J., Pujadas, M., Casuccio, G. S., Lersch, T. L., and Artíñano, B.: Individual  
599 particle characteristics of North African dust under different long-range transport scenarios, *Atmos.*  
600 *Environ.*, 43, 1850-1863, 10.1016/j.atmosenv.2008.12.045, 2009.

601 Coz, E., Artíñano, B., Clark, L. M., Hernandez, M., Robinson, A. L., Casuccio, G. S., Lersch, T. L., and  
602 Pandis, S. N.: Characterization of fine primary biogenic organic aerosol in an urban area in the  
603 northeastern United States, *Atmos. Environ.*, 44, 3952-3962,  
604 <https://doi.org/10.1016/j.atmosenv.2010.07.007>, 2010.

605 Crawford, I., Robinson, N. H., Flynn, M. J., Foot, V. E., Gallagher, M. W., Huffman, J. A., Stanley, W.  
606 R., and Kaye, P. H.: Characterisation of bioaerosol emissions from a Colorado pine forest: results from  
607 the BEACHON-RoMBAS experiment, *Atmos. Chem. Phys.*, 14, 8559-8578, 10.5194/acp-14-8559-2014,  
608 2014.

609 Crawford, I., Ruske, S., Topping, D. O., and Gallagher, M. W.: Evaluation of hierarchical agglomerative  
610 cluster analysis methods for discrimination of primary biological aerosol, *Atmos. Meas. Tech.*, 8, 4979-  
611 4991, 10.5194/amt-8-4979-2015, 2015.

612 Després, V., Huffman, J. A., Burrows, S. M., Hoose, C., Safatov, A., Buryak, G., Fröhlich-Nowoisky, J.,

613 Elbert, W., Andreae, M., Pöschl, U., and Jaenicke, R.: Primary biological aerosol particles in the  
614 atmosphere: a review, *Tellus B*, 64, 15598, 10.3402/tellusb.v64i0.15598, 2012.

615 Elbert, W., Taylor, P. E., Andreae, M. O., and Pöschl, U.: Contribution of fungi to primary biogenic  
616 aerosols in the atmosphere: wet and dry discharged spores, carbohydrates, and inorganic ions, *Atmos.*  
617 *Chem. Phys.*, 7, 4569-4588, 10.5194/acp-7-4569-2007, 2007.

618 Fröhlich-Nowoisky, J., Pickersgill, D. A., Després, V. R., and Pöschl, U.: High diversity of fungi in air  
619 particulate matter, *P. Natl. Acad. Sci.*, 106, 12814-12819, 10.1073/pnas.0811003106, 2009.

620 Gabey, A. M., Gallagher, M. W., Whitehead, J., Dorsey, J. R., Kaye, P. H., and Stanley, W. R.:  
621 Measurements and comparison of primary biological aerosol above and below a tropical forest canopy  
622 using a dual channel fluorescence spectrometer, *Atmos. Chem. Phys.*, 10, 4453-4466, 10.5194/acp-10-  
623 4453-2010, 2010.

624 Georgakopoulos, D. G., Després, V., Fröhlich-Nowoisky, J., Psenner, R., Ariya, P. A., Pósfai, M., Ahern,  
625 H. E., Moffett, B. F., and Hill, T. C. J.: Microbiology and atmospheric processes: biological, physical and  
626 chemical characterization of aerosol particles, *Biogeosciences*, 6, 721-737, 10.5194/bg-6-721-2009,  
627 2009.

628 Gosselin, M. I., Rathnayake, C. M., Crawford, I., Pöhlker, C., Fröhlich-Nowoisky, J., Schmer, B.,  
629 Després, V. R., Engling, G., Gallagher, M., Stone, E., Pöschl, U., and Huffman, J. A.: Fluorescent  
630 bioaerosol particle, molecular tracer, and fungal spore concentrations during dry and rainy periods in a  
631 semi-arid forest, *Atmos. Chem. Phys.*, 16, 15165-15184, 10.5194/acp-16-15165-2016, 2016.

632 Graham, B., Guyon, P., Maenhaut, W., Taylor, P. E., Ebert, M., Matthias-Maser, S., Mayol-Bracero, O.  
633 L., Godoi, R. H. M., Artaxo, P., Meixner, F. X., Moura, M. A. L., Rocha, C. H. E. D. A., Grieken, R. V.,  
634 Glovsky, M. M., Flagan, R. C., and Andreae, M. O.: Composition and diurnal variability of the natural  
635 Amazonian aerosol, *J. Geophy. Res.*, 108, 4765, doi:10.1029/2003JD004049, 2003.

636 Harrison, R. M., Jones, A. M., Biggins, P. D. E., Pomeroy, N., Cox, C. S., Kidd, S. P., Hobman, J. L.,  
637 Brown, N. L., and Beswick, A.: Climate factors influencing bacterial count in background air samples,  
638 *Int. J. Biometeorol.* 49, 167-178, 10.1007/s00484-004-0225-3, 2005.

639 Hu, W., Murata, K., Fukuyama, S., Kawai, Y., Oka, E., Uematsu, M., and Zhang, D.: Concentration and  
640 Viability of Airborne Bacteria Over the Kuroshio Extension Region in the Northwestern Pacific Ocean:  
641 Data From Three Cruises, *J. Geophy. Res.*, 122, 12,892-812,905, 10.1002/2017JD027287, 2017.

642 Hu, W., Niu, H., Murata, K., Wu, Z., Hu, M., Kojima, T., and Zhang, D.: Bacteria in atmospheric waters:  
643 Detection, characteristics and implications, *Atmos. Environ.*, 179, 201-221,  
644 <https://doi.org/10.1016/j.atmosenv.2018.02.026>, 2018.

645 Huffman, J. A., Treutlein, B., and Pöschl, U.: Fluorescent biological aerosol particle concentrations and  
646 size distributions measured with an Ultraviolet Aerodynamic Particle Sizer (UV-APS) in Central Europe,  
647 *Atmos. Chem. Phys.*, 10, 3215-3233, 10.5194/acp-10-3215-2010, 2010.

648 Huffman, J. A., Sinha, B., Garland, R. M., Snee-Pollmann, A., Gunthe, S. S., Artaxo, P., Martin, S. T.,  
649 Andreae, M. O., and Pöschl, U.: Size distributions and temporal variations of biological aerosol particles  
650 in the Amazon rainforest characterized by microscopy and real-time UV-APS fluorescence techniques  
651 during AMAZE-08, *Atmos. Chem. Phys.*, 12, 11997-12019, 10.5194/acp-12-11997-2012, 2012.

652 Huffman, J. A., Prenni, A. J., DeMott, P. J., Pöhlker, C., Mason, R. H., Robinson, N. H., Fröhlich-  
653 Nowoisky, J., Tobo, Y., Després, V. R., Garcia, E., Gochis, D. J., Harris, E., Müller-Germann, I., Ruzene,  
654 C., Schmer, B., Sinha, B., Day, D. A., Andreae, M. O., Jimenez, J. L., Gallagher, M., Kreidenweis, S. M.,  
655 Bertram, A. K., and Pöschl, U.: High concentrations of biological aerosol particles and ice nuclei during  
656 and after rain, *Atmos. Chem. Phys.*, 13, 6151-6164, 10.5194/acp-13-6151-2013, 2013.

657 Lacey, M. E., and West, J. S.: The Air Spora: A Manual for Catching and Identifying Airborne Biological  
658 Particles, Springer: Dordrecht, The Netherlands, 2006.

659 Lee, B. U., Kim, S. H., and Kim, S. S.: Hygroscopic growth of *E. coli* and *B. subtilis* bioaerosols, *J.*  
660 *Aerosol Sci.*, 33, 1721-1723, [https://doi.org/10.1016/S0021-8502\(02\)00114-3](https://doi.org/10.1016/S0021-8502(02)00114-3), 2002.

661 Li, W., Shao, L., Zhang, D., Ro, C.-U., Hu, M., Bi, X., Geng, H., Matsuki, A., Niu, H., and Chen, J.: A  
662 review of single aerosol particle studies in the atmosphere of East Asia: morphology, mixing state, source,  
663 and heterogeneous reactions, *J. Clean. Prod.*, 112, Part 2, 1330-1349, 2016.

664 Li, W., Xu, L., Liu, X., Zhang, J., Lin, Y., Yao, X., Gao, H., Zhang, D., Chen, J., Wang, W., Harrison, R.  
665 M., Zhang, X., Shao, L., Fu, P., Nenes, A., and Shi, Z.: Air pollution-aerosol interactions produce more  
666 bioavailable iron for ocean ecosystems, *Sci. Adv.*, 3, e1601749, 2017.

667 Ling, M. L., Wex, H., Grawe, S., Jakobsson, J., Löndahl, J., Hartmann, S., Finster, K., Boesen, T., and  
668 Šantl-Temkiv, T.: Effects of Ice Nucleation Protein Repeat Number and Oligomerization Level on Ice  
669 Nucleation Activity, *J. Geophys. Res.*, 123, 1802-1810, 10.1002/2017JD027307, 2018.

670 Möhler, O., DeMott, P. J., Vali, G., and Levin, Z.: Microbiology and atmospheric processes: the role of  
671 biological particles in cloud physics, *Biogeosciences*, 4, 1059-1071, 10.5194/bg-4-1059-2007, 2007.

672 Manninen, H. E., Back, J., Sihto-Nissila, S. L., Huffman, J. A., Pessi, A. M., Hiltunen, V., Aalto, P. P.,  
673 Hidalgo, P. J., Hari, P., Saarto, A., Kulmala, M., and Petaja, T.: Patterns in airborne pollen and other  
674 primary biological aerosol particles (PBAP), and their contribution to aerosol mass and number in a  
675 boreal forest, *Boreal Environ. Res.*, 19, 383-405, 2014.

676 Martin, S. T., Andreae, M. O., Artaxo, P., Baumgardner, D., Chen, Q., Goldstein, A. H., Guenther, A.,  
677 Heald, C. L., Mayol-Bracero, O. L., McMurry, P. H., Pauliquevis, T., Pochl, U., Prather, K. A., Roberts,  
678 G. C., Saleska, S. R., Silva Dias, M. A., Spracklen, D. V., Swietlicki, E., and Trebs, I.: Sources and  
679 properties of Amazonian aerosol particles, *Rev. Geophys.*, 48, RG2002, 10.1029/2008rg000280, 2010.

680 May, N. W., Olson, N. E., Panas, M., Axson, J. L., Tirella, P. S., Kirpes, R. M., Craig, R. L., Gunsch, M.  
681 J., China, S., Laskin, A., Ault, A. P., and Pratt, K. A.: Aerosol Emissions from Great Lakes Harmful  
682 Algal Blooms, *Environ. Sci. Technol.*, 52, 397-405, 10.1021/acs.est.7b03609, 2018.

683 Morris, C. E., Georgakopoulos, D. G., and Sands, D. C.: Ice nucleation active bacteria and their potential  
684 role in precipitation, *J. Phys. IV France*, 121, 87-103, 2004.

685 Morris, C. E., Conen, F., Alex Huffman, J., Phillips, V., Pöschl, U., and Sands, D. C.: Bioprecipitation: a  
686 feedback cycle linking Earth history, ecosystem dynamics and land use through biological ice nucleators  
687 in the atmosphere, *Global Change Biol.*, 20, 341-351, 10.1111/gcb.12447, 2014.

688 Nikkels, A. H., Terstegge, P., and Spieksma, F. T. M.: Ten types of microscopically identifiable airborne  
689 fungal spores at Leiden, The Netherlands, *Aerobiologia*, 12, 107, 10.1007/bf02446602, 1996.

690 Patterson, J. P., Collins, D. B., Michaud, J. M., Axson, J. L., Sultana, C. M., Moser, T., Dommer, A. C.,  
691 Conner, J., Grassian, V. H., Stokes, M. D., Deane, G. B., Evans, J. E., Burkart, M. D., Prather, K. A., and  
692 Gianneschi, N. C.: Sea Spray Aerosol Structure and Composition Using Cryogenic Transmission  
693 Electron Microscopy, *ACS Central Sci.*, 2, 40-47, 10.1021/acscentsci.5b00344, 2016.

694 Poschl, U.: Atmospheric aerosols: Composition, transformation, climate and health effects, *Angew.*  
695 *Chem. Int. Edit.*, 44, 7520-7540, 10.1002/anie.200501122, 2005.

696 Posfai, M., Li, J., Anderson, J. R., and Buseck, P. R.: Aerosol bacteria over the southern ocean during  
697 ACE-1, *Atmos. Res.*, 66, 231-240, 2003.

698 Pratt, K. A., DeMott, P. J., French, J. R., Wang, Z., Westphal, D. L., Heymsfield, A. J., Twohy, C. H.,  
699 Prenni, A. J., and Prather, K. A.: In situ detection of biological particles in cloud ice-crystals, *Nat. Geosci.*,  
700 2, 398-401, 2009.

701 Prenni, A. J., Petters, M. D., Kreidenweis, S. M., Heald, C. L., Martin, S. T., Artaxo, P., Garland, R. M.,  
702 Wollny, A. G., and Poschl, U.: Relative roles of biogenic emissions and Saharan dust as ice nuclei in the  
703 Amazon basin, *Nat. Geosci.*, 2, 402-405, 2009.

704 Priyamvada, H., Singh, R. K., Akila, M., Ravikrishna, R., Verma, R. S., and Gunthe, S. S.: Seasonal  
705 variation of the dominant allergenic fungal aerosols – One year study from southern Indian region,  
706 *Scientific Reports*, 7, 11171, 10.1038/s41598-017-11727-7, 2017.

707 Reponen, T., Willeke, K., Ulevicius, V., Reponen, A., and Grinshpun, S. A.: Effect of relative humidity  
708 on the aerodynamic diameter and respiratory deposition of fungal spores, *Atmos. Environ.*, 30, 3967-  
709 3974, [https://doi.org/10.1016/1352-2310\(96\)00128-8](https://doi.org/10.1016/1352-2310(96)00128-8), 1996.

710 Riemer, N., Ault, A. P., West, M., Craig, R. L., and Curtis, J. H.: Aerosol Mixing State: Measurements,  
711 Modeling, and Impacts, *Rev. Geophys.*, 57, <https://doi.org/10.1029/2018RG000615>,  
712 10.1029/2018rg000615, 2019.

713 Rissler, J., Vestin, A., Swietlicki, E., Fisch, G., Zhou, J., Artaxo, P., and Andreae, M. O.: Size distribution  
714 and hygroscopic properties of aerosol particles from dry-season biomass burning in Amazonia, *Atmos.*  
715 *Chem. Phys.*, 6, 471-491, 10.5194/acp-6-471-2006, 2006.

716 Shi, Z., Shao, L., Jones, T. P., Whittaker, A. G., Lu, S., Berube, K. A., He, T., and Richards, R. J.:  
717 Characterization of airborne individual particles collected in an urban area, a satellite city and a clean air  
718 area in Beijing, 2001, *Atmos. Environ.*, 37, 4097-4108, 2003.

719 Shi, Z., He, K., Xue, Z., Yang, F., Chen, Y., Ma, Y., and Luo, J.: Properties of individual aerosol particles  
720 and their relation to air mass origins in a south China coastal city, *J. Geophy. Res.*, 114,  
721 doi:10.1029/2008JD011221, 2009.

722 Smith, D. J., Ravichandar, J. D., Jain, S., Griffin, D. W., Yu, H., Tan, Q., Thissen, J., Lusby, T., Nicoll,  
723 P., Shedler, S., Martinez, P., Osorio, A., Lechniak, J., Choi, S., Sabino, K., Iverson, K., Chan, L., Jaing,  
724 C., and McGrath, J.: Airborne Bacteria in Earth's Lower Stratosphere Resemble Taxa Detected in the  
725 Troposphere: Results From a New NASA Aircraft Bioaerosol Collector (ABC), *Front. Microbiol.* 9,  
726 10.3389/fmicb.2018.01752, 2018.

727 Spracklen, D. V., Bonn, B., and Carslaw, K. S.: Boreal forests, aerosols and the impacts on clouds and  
728 climate, *Philos. T. R. Soc. A.*, 366, 4613-4626, 10.1098/rsta.2008.0201, 2008.

729 Sun, J., Liu, L., Xu, L., Wang, Y., Wu, Z., Hu, M., Shi, Z., Li, Y., Zhang, X., Chen, J., and Li, W.: Key  
730 Role of Nitrate in Phase Transitions of Urban Particles: Implications of Important Reactive Surfaces for  
731 Secondary Aerosol Formation, *J. Geophy. Res.*, 123, 1234-1243, 10.1002/2017JD027264, 2018.

732 Tamer Vestlund, A., Al-Ashaab, R., Tyrrel, S. F., Longhurst, P. J., Pollard, S. J. T., and Drew, G. H.:  
733 Morphological classification of bioaerosols from composting using scanning electron microscopy, *Waste  
734 Manage.*, 34, 1101-1108, <https://doi.org/10.1016/j.wasman.2014.01.021>, 2014.

735 Therkorn, J., Thomas, N., Scheinbeim, J., and Mainelis, G.: Field performance of a novel passive  
736 bioaerosol sampler using polarized ferroelectric polymer films, *Aerosol Sci. Tech.*, 51, 787-800,  
737 10.1080/02786826.2017.1316830, 2017.

738 Tobo, Y., Prenni, A. J., DeMott, P. J., Huffman, J. A., McCluskey, C. S., Tian, G., Pöhlker, C., Pöschl, U.,  
739 and Kreidenweis, S. M.: Biological aerosol particles as a key determinant of ice nuclei populations in a  
740 forest ecosystem, *J. Geophy. Res.*, 118, 10,100-110,110, 10.1002/jgrd.50801, 2013.

741 Tong, Y., and Lighthart, B.: The Annual Bacterial Particle Concentration and Size Distribution in the  
742 Ambient Atmosphere in a Rural Area of the Willamette Valley, Oregon, *Aerosol Sci. Techn.*, 32, 393-  
743 403, 10.1080/027868200303533, 2000.

744 Toprak, E., and Schnaiter, M.: Fluorescent biological aerosol particles measured with the Waveband

745 Integrated Bioaerosol Sensor WIBS-4: laboratory tests combined with a one year field study, *Atmos.*  
746 *Chem. Phys.*, 13, 225-243, 10.5194/acp-13-225-2013, 2013.

747 Troutt, C., and Levettin, E.: Correlation of spring spore concentrations and meteorological conditions in  
748 Tulsa, Oklahoma, *Int. J. Biometeorol.*, 45, 64-74, 10.1007/s004840100087, 2001.

749 Tunved, P., Hansson, H.-C., Kerminen, V.-M., Ström, J., Maso, M. D., Lihavainen, H., Viisanen, Y.,  
750 Aalto, P. P., Komppula, M., and Kulmala, M.: High Natural Aerosol Loading over Boreal Forests, *Science*,  
751 312, 261-263, 10.1126/science.1123052, 2006.

752 Twohy, C. H., McMeeking, G. R., DeMott, P. J., McCluskey, C. S., Hill, T. C. J., Burrows, S. M., Kulkarni,  
753 G. R., Tanarhte, M., Kafle, D. N., and Toohey, D. W.: Abundance of fluorescent biological aerosol  
754 particles at temperatures conducive to the formation of mixed-phase and cirrus clouds, *Atmos. Chem.*  
755 *Phys.*, 16, 8205-8225, 10.5194/acp-16-8205-2016, 2016.

756 Valsan, A. E., Priyamvada, H., Ravikrishna, R., Després, V. R., Biju, C. V., Sahu, L. K., Kumar, A.,  
757 Verma, R. S., Philip, L., and Gunthe, S. S.: Morphological characteristics of bioaerosols from contrasting  
758 locations in southern tropical India – A case study, *Atmos. Environ.*, 122, 321-331,  
759 <https://doi.org/10.1016/j.atmosenv.2015.09.071>, 2015.

760 Valsan, A. E., Ravikrishna, R., Biju, C. V., Pöhlker, C., Després, V. R., Huffman, J. A., Pöschl, U., and  
761 Gunthe, S. S.: Fluorescent biological aerosol particle measurements at a tropical high-altitude site in  
762 southern India during the southwest monsoon season, *Atmos. Chem. Phys.*, 16, 9805-9830, 10.5194/acp-  
763 16-9805-2016, 2016.

764 Whitehead, J. D., Derbyshire, E., Brito, J., Barbosa, H. M. J., Crawford, I., Stern, R., Gallagher, M. W.,  
765 Kaye, P. H., Allan, J. D., Coe, H., Artaxo, P., and McFiggans, G.: Biogenic cloud nuclei in the central  
766 Amazon during the transition from wet to dry season, *Atmos. Chem. Phys.*, 16, 9727-9743, 10.5194/acp-  
767 16-9727-2016, 2016.

768 Wilson, T. W., Ladino, L. A., Alpert, P. A., Breckels, M. N., Brooks, I. M., Browne, J., Burrows, S. M.,  
769 Carslaw, K. S., Huffman, J. A., Judd, C., Kilthau, W. P., Mason, R. H., McFiggans, G., Miller, L. A.,  
770 Nájera, J. J., Polishchuk, E., Rae, S., Schiller, C. L., Si, M., Temprado, J. V., Whale, T. F., Wong, J. P. S.,  
771 Wurl, O., Yakobi-Hancock, J. D., Abbatt, J. P. D., Aller, J. Y., Bertram, A. K., Knopf, D. A., and Murray,  
772 B. J.: A marine biogenic source of atmospheric ice-nucleating particles, *Nature*, 525, 234,  
773 10.1038/nature14986, 2015.

774 Wittmaack, K.: Brochosomes produced by leafhoppers-a widely unknown, yet highly abundant species  
775 of bioaerosols in ambient air, *Atmos. Environ.*, 39, 1173-1180,  
776 <https://doi.org/10.1016/j.atmosenv.2004.11.003>, 2005.

777 Wittmaack, K., Wehnes, H., Heinemann, U., and Agerer, R.: An overview on bioaerosols viewed by  
778 scanning electron microscopy, *Sci. Total Environ.*, 346, 244-255,  
779 <https://doi.org/10.1016/j.scitotenv.2004.11.009>, 2005.

780 Wu, L., Li, X., Kim, H., Geng, H., Godoi, R. H. M., Barbosa, C. G. G., Godoi, A. F. L., Yamamoto, C.  
781 I., de Souza, R. A. F., Pöhlker, C., Andreae, M. O., and Ro, C. U.: Single-particle characterization of  
782 aerosols collected at a remote site in the Amazonian rainforest and an urban site in Manaus, Brazil, *Atmos.*  
783 *Chem. Phys.*, 19, 1221-1240, 10.5194/acp-19-1221-2019, 2019.

784 Yue, S., Ren, H., Fan, S., Wei, L., Zhao, J., Bao, M., Hou, S., Zhan, J., Zhao, W., Ren, L., Kang, M., Li,  
785 L., Zhang, Y., Sun, Y., Wang, Z., and Fu, P.: High Abundance of Fluorescent Biological Aerosol Particles  
786 in Winter in Beijing, China, *ACS Earth Space Chem.*, 1, 493-502, 10.1021/acsearthspacechem.7b00062,  
787 2017.

788 Zawadowicz, M. A., Froyd, K. D., Murphy, D. M., and Cziczo, D. J.: Improved identification of primary

789 biological aerosol particles using single-particle mass spectrometry, *Atmos. Chem. Phys.*, 17, 7193-7212,  
790 10.5194/acp-17-7193-2017, 2017.

791 Zhang, D., Murata, K., Hu, W., Yuan, H., Li, W., Matsusaki, H., and Kakikawa, M.: Concentration and  
792 Viability of Bacterial Aerosols Associated with Weather in Asian Continental Outflow: Current  
793 Understanding, *Aerosol Sci. Engin.*, 1-12, 10.1007/s41810-017-0008-y, 2017.

# Supplemental Materials

## **Overview of primary biological aerosol particles from a Chinese boreal forest: insight into morphology, size, and mixing state at microscopic scale**

Weijun Li<sup>1</sup>, Lei Liu<sup>1</sup>, Qi Yuan<sup>1</sup>, Liang Xu<sup>1</sup>, Yanhong Zhu<sup>1</sup>, Bingbing Wang<sup>2</sup>, Hua Yu<sup>3</sup>, Xiaokun Ding<sup>4</sup>, Jian Zhang<sup>1</sup>, Dao Huang<sup>1</sup>, Dantong Liu<sup>1</sup>, Wei Hu<sup>5</sup>, Daizhou Zhang<sup>6</sup>, Pingqing Fu<sup>5</sup>, Maosheng Yao<sup>7</sup>, Min Hu<sup>7</sup>, Xiaoye Zhang<sup>8</sup>, Zongbo Shi<sup>9,5</sup>

<sup>1</sup>Department of Atmospheric Sciences, School of Earth Sciences, Zhejiang University, Hangzhou 310027, China

<sup>2</sup>State Key Laboratory of Marine Environmental Science, College of Ocean and Earth Sciences, Xiamen University, Xiamen 361102, China.

<sup>3</sup>College of Life and Environmental Sciences, Hangzhou Normal University, 310036, Hangzhou, China

<sup>4</sup>Department of Chemistry, Zhejiang University, Hangzhou 310027, China

<sup>5</sup>Institute of Surface-Earth System Science, Tianjin University, 300072, Tianjin, China

<sup>6</sup>Faculty of Environmental and Symbiotic Sciences, Prefectural University of Kumamoto, Kumamoto 862-8502, Japan

<sup>7</sup>State Key Joint Laboratory of Environmental Simulation and Pollution Control, College of Environmental Sciences and Engineering, Peking University, Beijing 100871, China

<sup>8</sup>Key Laboratory of Atmospheric Chemistry, Chinese Academy of Meteorological Sciences, Beijing, China

<sup>9</sup>School of Geography, Earth and Environmental Sciences, University of Birmingham,  
Birmingham B15 2TT, UK

*\*Correspondence to:* Weijun Li (liweijun@zju.edu.cn)

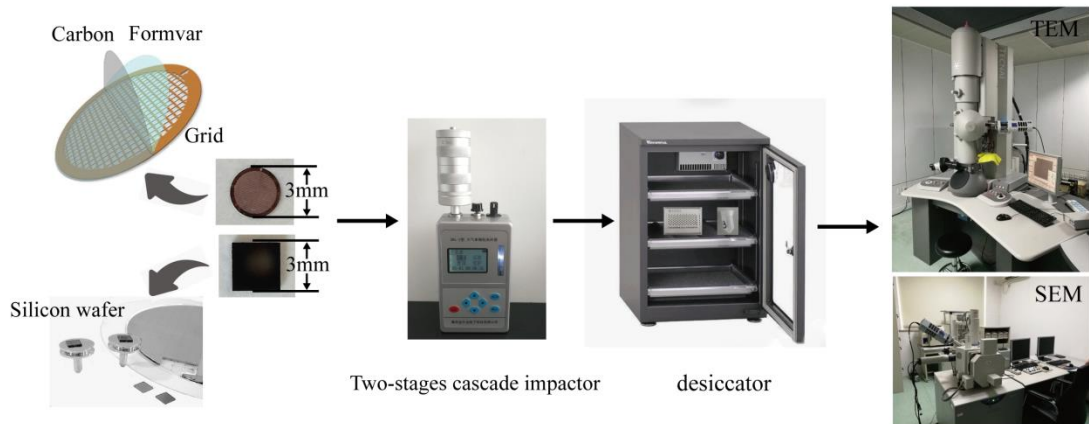


**Figure S1** The sampling procedures of substrate, sampler, storage, and analyzed technique.

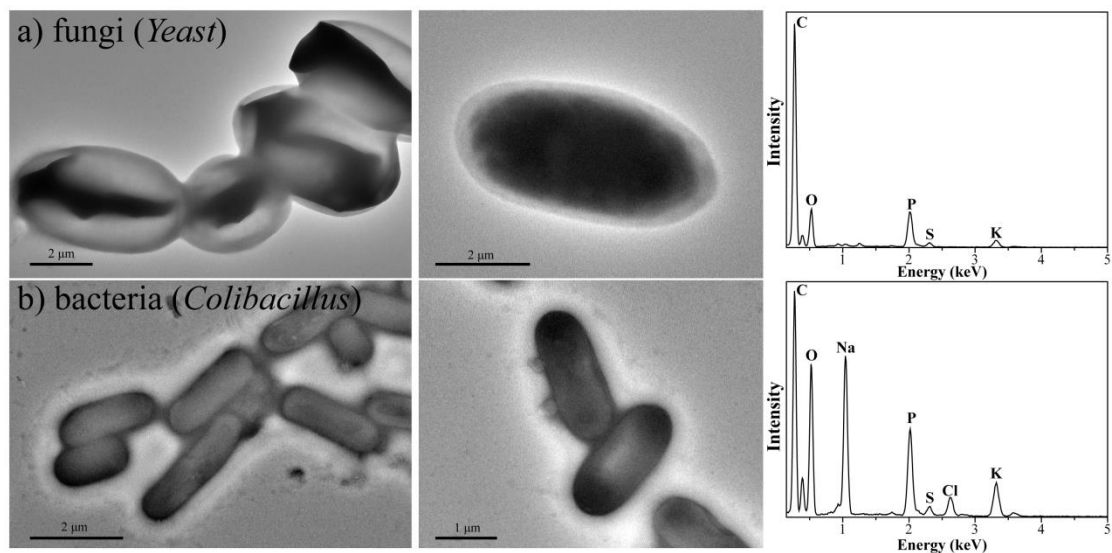


**Figure S2** The *Yeast* and the *colibacillus* particles cultivated in laboratory. TEM image showing morphology and EDS showing compositions.

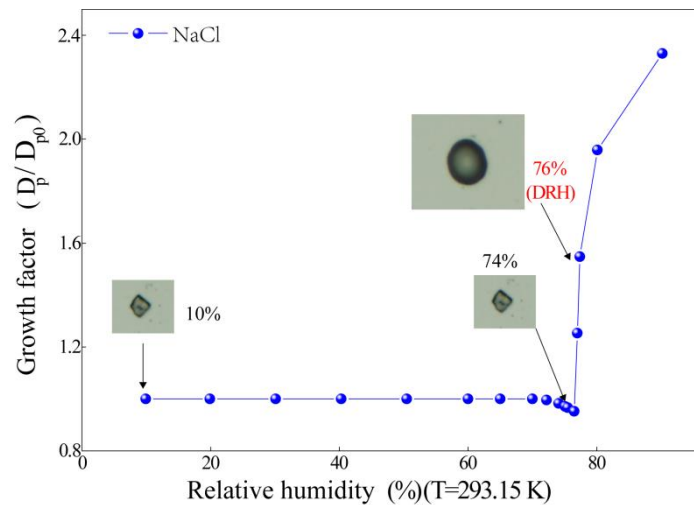


**Figure S3** Hygroscopic growth of NaCl generated in laboratory

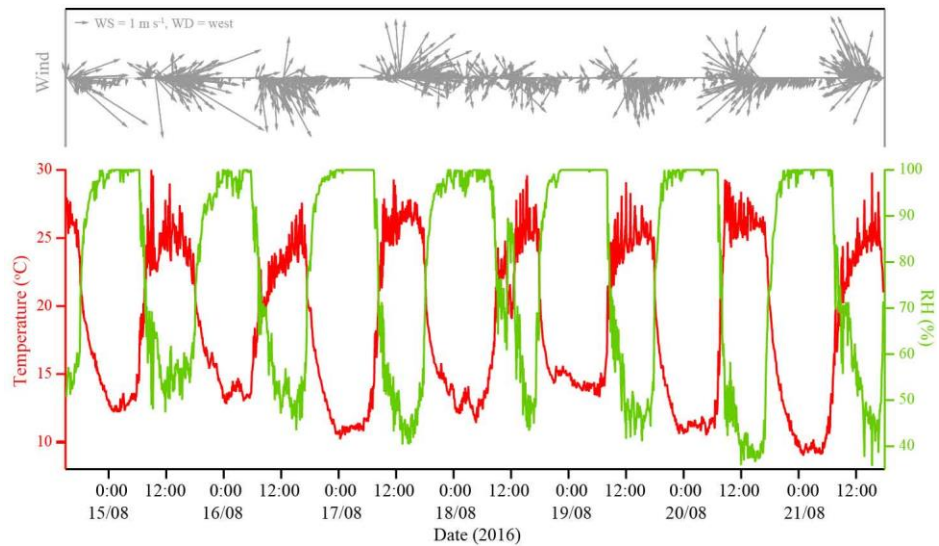


**Figure S4** Meteorological data during the sampling including Wind speed and direction, Temperature, and relative humidity (RH).

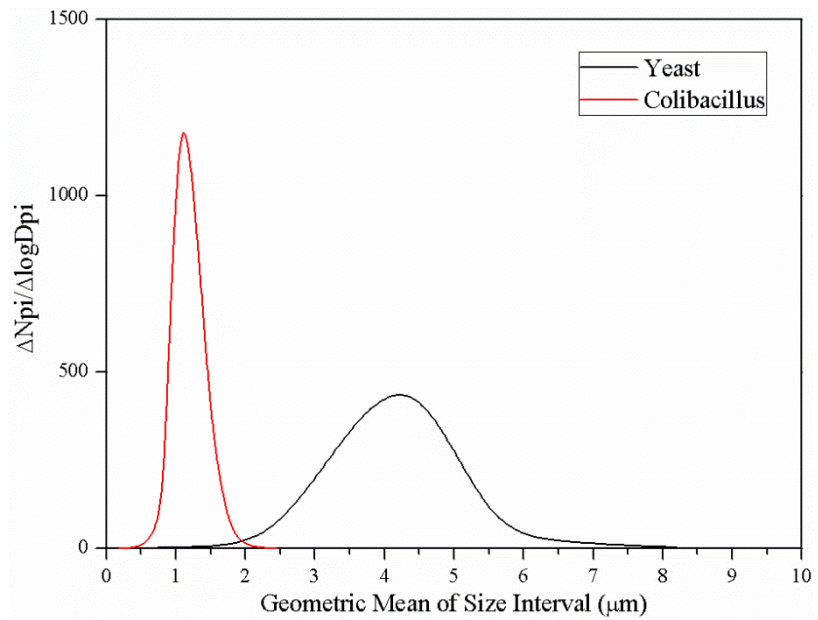


**Figure S5** Size distribution of Yeast and Colibacillus cultivated in laboratory.

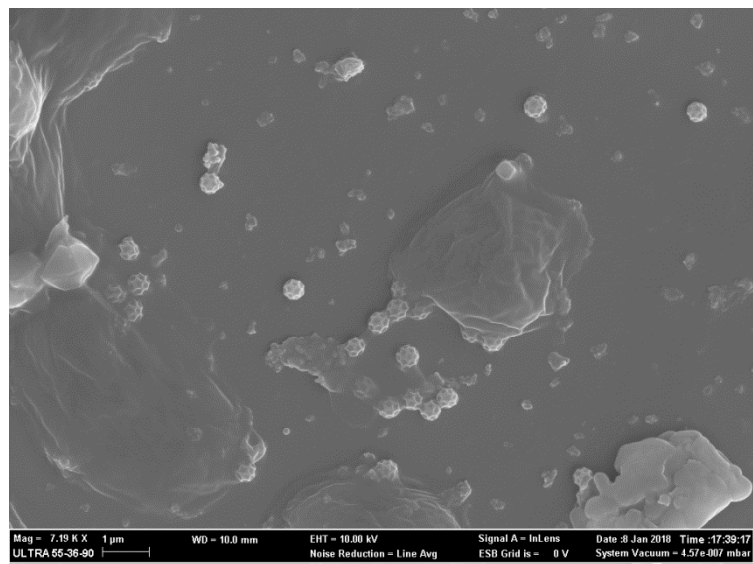


**Figure S6** SEM images of brochosomes.

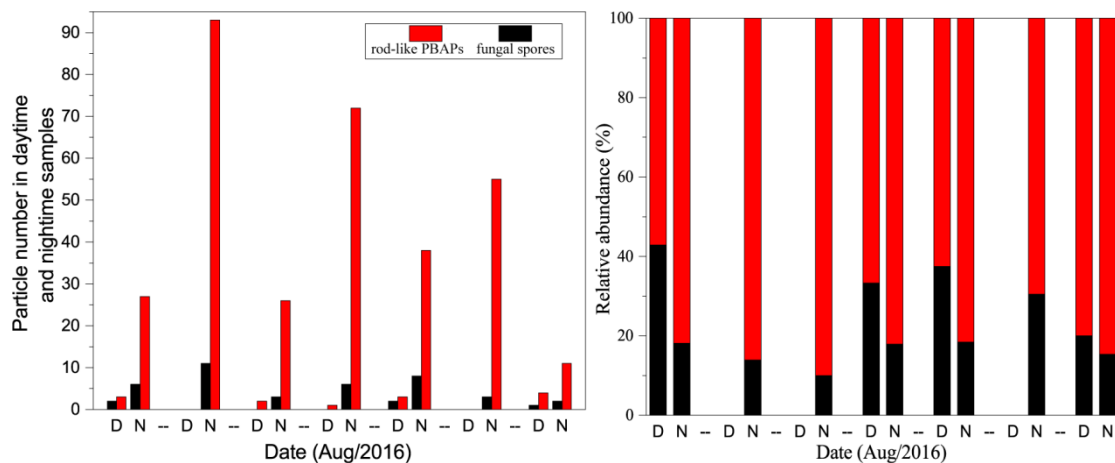


**Figure S7** Particle number and relative abundance of rod-like PBAPs and fungal spores in the samples collected in daytime and nighttime.